Supporting Information

Dual Inhibition of Human Parainfluenza Type 3 and Respiratory Syncytial Virus Infectivity with a Single Agent

Victor K. Outlaw[1], Samantha Bottom-Tanzer[2,3], Dale F. Kreitler[1], Samuel H. Gellman[1], Matteo Porotto[2,3,4], Anne Moscona[2,3,5,6*]

[1] Department of Chemistry, University of Wisconsin, Madison, Wisconsin, 53706, United States

[2] Department of Pediatrics, Columbia University Medical Center, New York, New York, 10032, United States

[3] Center for Host–Pathogen Interaction, Columbia University Medical Center, New York, New York, 10032, United States

[4] Department of Experimental Medicine, University of Campania 'Luigi Vanvitelli', Italy

[5] Department of Microbiology & Immunology, Columbia University Medical Center, New York, New York, 10032, United States

[6] Department of Physiology & Cellular Biophysics, Columbia University Medical Center, New York, New York, 10032, United States

[*] Corresponding Author. Address correspondence to: Anne Moscona, am939@cumc.columbia.edu

Table of Contents

Peptide Synthesis and Purification

Instrumentation

Solid-phase peptide synthesis was performed on a CEM MARS microwave reactor using polypropylene syringes fitted with a porous disc (Torviq). Preparative HPLC was performed using a Shimadzu HPLC system (SCL-10VP system controller, LC-6AD pumps, SIL-10ADVP autosampler, SPD-10VP UV-vis detector, FRC-10A fraction collector) equipped with a Waters XSelect CSH Prep C18 column (5 μm particle size, 19 mm × 250 mm). Peptide purity measurements were performed on a Waters Acquity H-Class UPLC equipped with an Acquity UPLC BEH C18 column (130 Å pore size, 1.7 μm particle size, 2.1 mm × 50 mm). Mass spectra were obtained on a Bruker microflex LRF MALDI-TOF-MS. Circular dichroism experiments were performed on an Aviv Biomedical model 420 CD spectrometer.

Instrument Name	**Instrument Type**	**Grant**
Waters Acquity H-Class	UPLC	DARPA N66001-15-2-4023
Bruker microflex LRF	MALDI-TOF-MS	Generous gift from the Bender Fund
Aviv Biomedical model 420	CD spectrometer	NIH R01GM056414

General Procedure

Peptides were prepared on Rink amide resin using microwave-assisted solid-phase peptide synthesis (MA-SPPS). Resin was purchased from Millipore–Sigma. Fmoc-amino acids and coupling reagents were purchased from Chem-Impex International. Protected Fmoc-α-amino acids included: Asp(*t*-Bu ester), Glu(*t*-Bu ester), His(trityl), Lys(Boc), Asn(trityl), Gln(trityl), Arg(Pbf), Ser(*t*-Bu ether), Thr(*t*-Bu ether), Trp(Boc), and Tyr(*t*-Bu ether).

Rink amide resin was pre-swelled with DMF in a polypropylene fritted syringe, then drained and washed with DMF. Coupling reactions were performed using solutions comprised of 4 equivalents Fmoc-amino acid, 4 equivalents of 1-[bis(dimethylamino)methylene]-1H-1,2,3-triazolo[4,5-b]pyridinium 3-oxide hexafluorophosphate (HATU), and 8 equivalents of diisopropylethylamine (DIEA) in biotechnology-grade dimethylformamide (DMF) at a final concentration of 100 mM Fmoc-amino acid. Coupling reactions were carried out by microwave-assisted synthesis using a 2 min ramp to 70 °C followed by a 4 min hold at 70 °C. Deprotection was effected by addition of 20% (v/v) piperidine in biotechnology-grade DMF. The deprotection reactions were carried out by microwave-assisted

synthesis using a 2 min ramp to 80 °C followed by a 2 min hold at 80 °C. The resin was washed with 3–5 resin volumes of biotechnology-grade DMF after each coupling and deprotection reaction.

HPIV3 HRN and RSV HRN could not be prepared by standard MS-SPPS. We presume that coupling inefficiency was due to the extensive lengths and hydrophobicities of these sequences. To prevent on-resin aggregation, pseudoproline dipeptides (Millipore-Sigma, underlined in the sequences below) were incorporated at strategic positions throughout the sequence, which resulted in successful syntheses.

HPIV3 HRN: Ac-QARSDIEKLKEAIRDTNKAVQSVQSSIGNLIVAIKSVQDYVNKEIVPSIAR-NH_2

RSV HRN: Ac-HLEGEVNKIKSALLSTNKAVVSLSNGVSVLTSKVLDLKNYIDKQLLPIVNK -NH_2

Following the final deprotection step, the N-terminus of the peptide was capped by stirring in 8:2:1 DMF:DIEA:Ac_2O at 23 °C for 30 minutes. The resin was washed with DMF and DCM, and peptide cleavage from resin was effected by mixing with a solution of 94% TFA, 2.5% ethanedithiol, 2.5% H_2O, and 1% triisopropylsilane for 3 hours. The resulting solution was filtered through the fritted syringe, the remaining resin was washed with 2–3 column volumes of TFA, and the combined extracts were concentrated under N_2. The peptide was precipitated by addition of cold diethyl ether, pelleted by centrifugation, and dried under N_2 to afford a crude powder. Purification of peptides was achieved by reverse-phase HPLC on a semi-preparative C18 column using a gradient of water (+0.1% TFA) and acetonitrile (+0.1% TFA). The identity of each peptide was confirmed by MALDI-TOF mass spectrometry. Purity was established by peak area integration of reverse phase UPLC chromatograms using a 10–95% H_2O/MeCN (+0.1% TFA) gradient over 6 minutes (Figures S1–S32).

N-Terminal Heptad Repeat Domain of HPIV3 F (HPIV3 HRN)

Sequence: Ac-QARSDIEKLKEAIRDTNKAVQSVQSSIGNLIVAIKSVQDYVNKEIVPSIAR-NH_2

Calculated monoisotopic [M+H]: 5663.1

Calculated monoisotopic [M+2H]: 2832.1

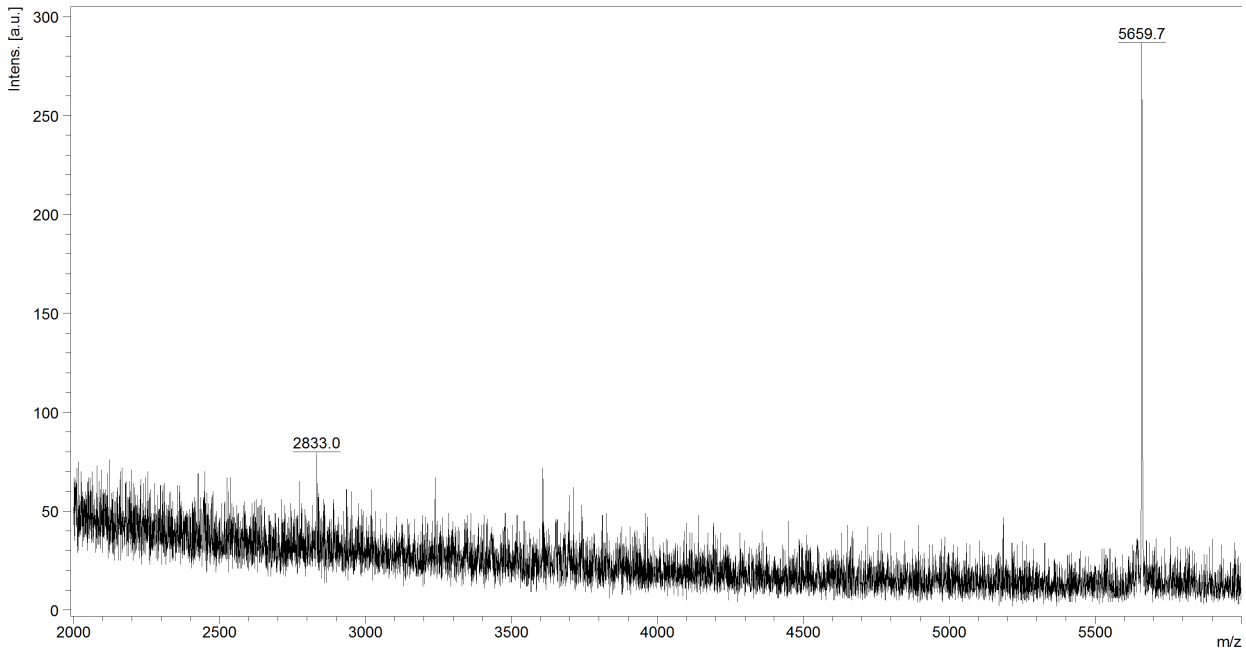

Figure S1. HPIV3 HRN MALDI-TOF analysis

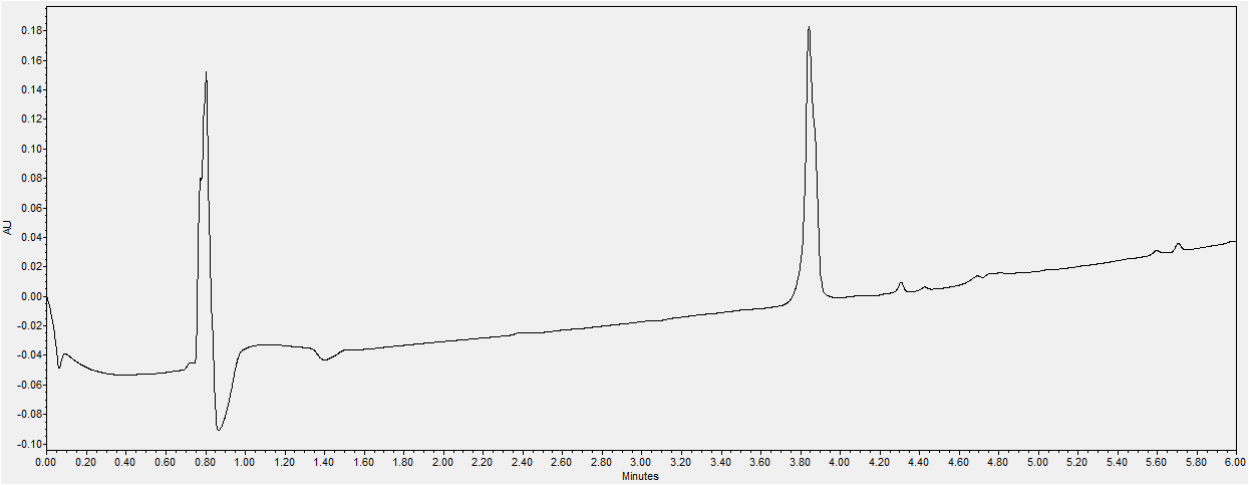

Figure S2. HPIV3 HRN UPLC purity analysis, UPLC gradient from 10-95% MeCN/H_2O over 6 minutes (0.3 mL/min; column-Waters Acquity BEH C4 1.7 μm, 2.1 x 100 mm, purity >95%)

N-Terminal Heptad Repeat Domain of RSV F (RSV HRN)

Sequence: Ac-HLEGEVNKIKSALLSTNKAVVSLSNGVSVLTSKVLDLKNYIDKQLLPIVNK -NH_2

Calculated monoisotopic [M+H]: 5571.2

Calculated monoisotopic [M+2H]: 2786.1

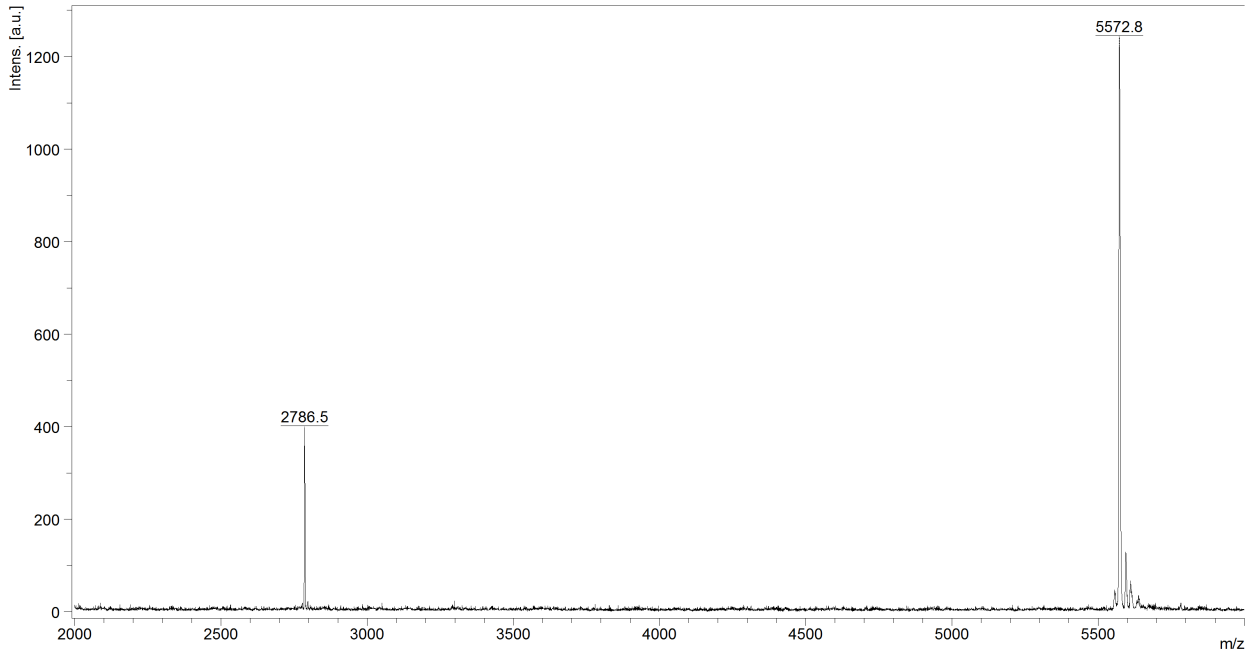

Figure S3. RSV HRN MALDI-TOF analysis

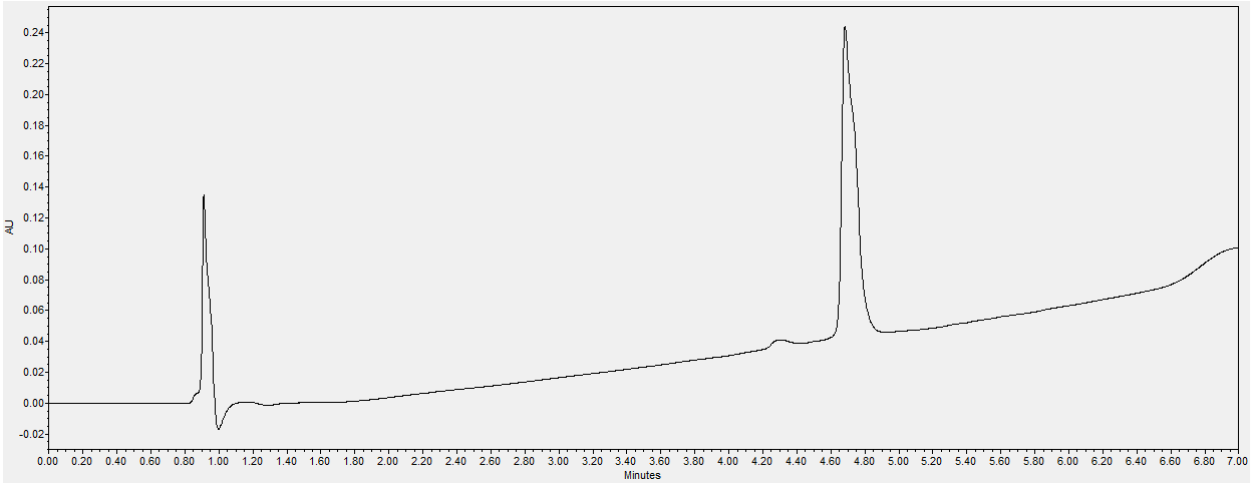

Figure S4. RSV HRN UPLC purity analysis, UPLC gradient from 10-95% MeCN/H_2O over 6 minutes (0.3 mL/min; column-Waters Acquity BEH C4 1.7 μm, 2.1 x 100 mm, purity >95%)

C-Terminal Heptad Repeat Domain of HPIV3 F (HPIV3 HRC)

Sequence: Ac-VALDPIDISIELNKAKSDLEESKEWIRRSNQKLDSI -NH_2

Calculated monoisotopic [M+H]: 4194.2

Calculated monoisotopic [M+2H]: 2097.6

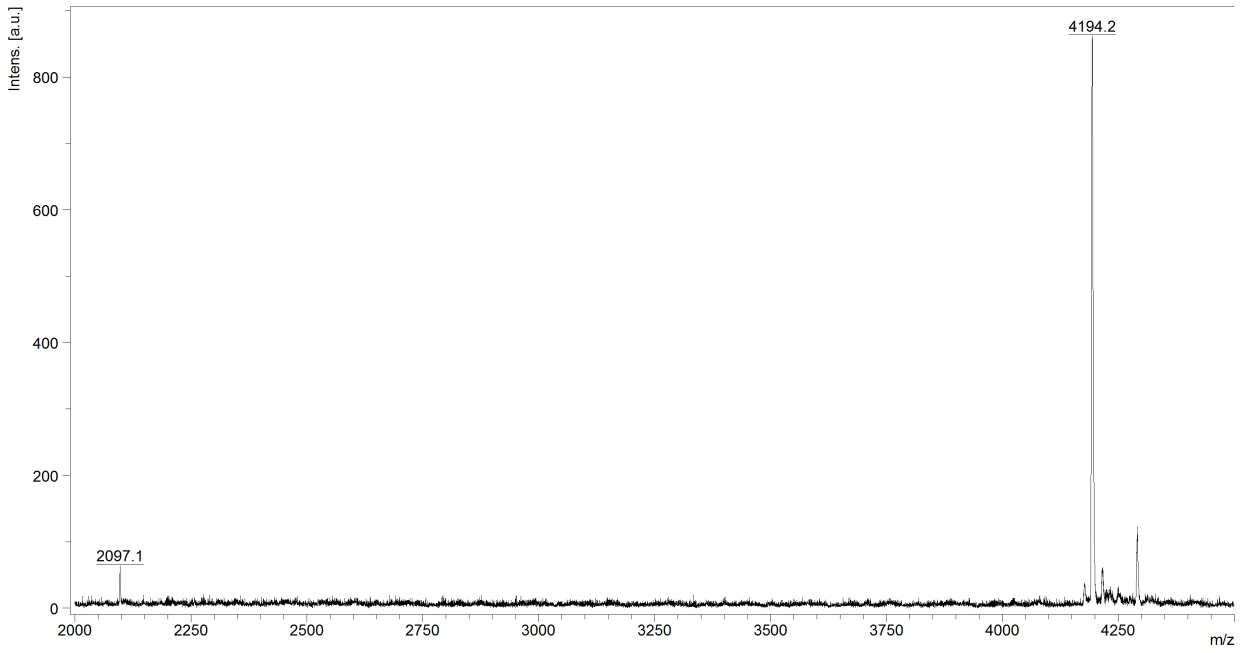

Figure S5. HPIV3 HRC MALDI-TOF analysis

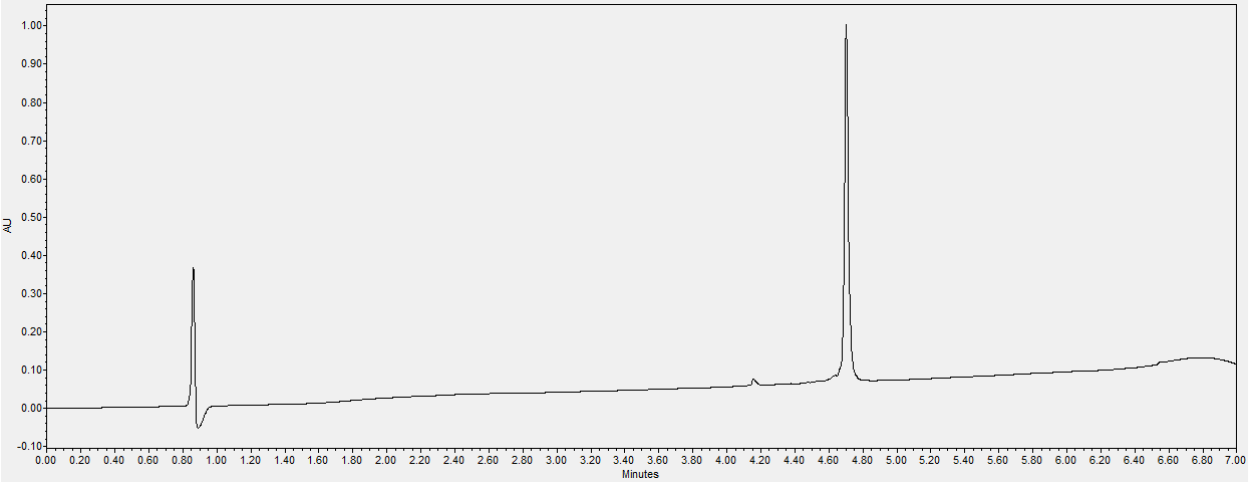

Figure S6. HPIV3 HRC UPLC purity analysis, UPLC gradient from 10-95% MeCN/H_2O over 6 minutes (0.3 mL/min; column-Waters Acquity BEH C4 1.7 µm, 2.1 x 100 mm, purity >95%)

C-Terminal Heptad Repeat Domain of RSV F (RSV HRC)

Sequence: Ac-LVFPSDEFDASISQVNEKINQSLAFIRKSDELLHNV-NH_2

Calculated monoisotopic [M+H]: 4144.1

Calculated monoisotopic [M+2H]: 2072.6

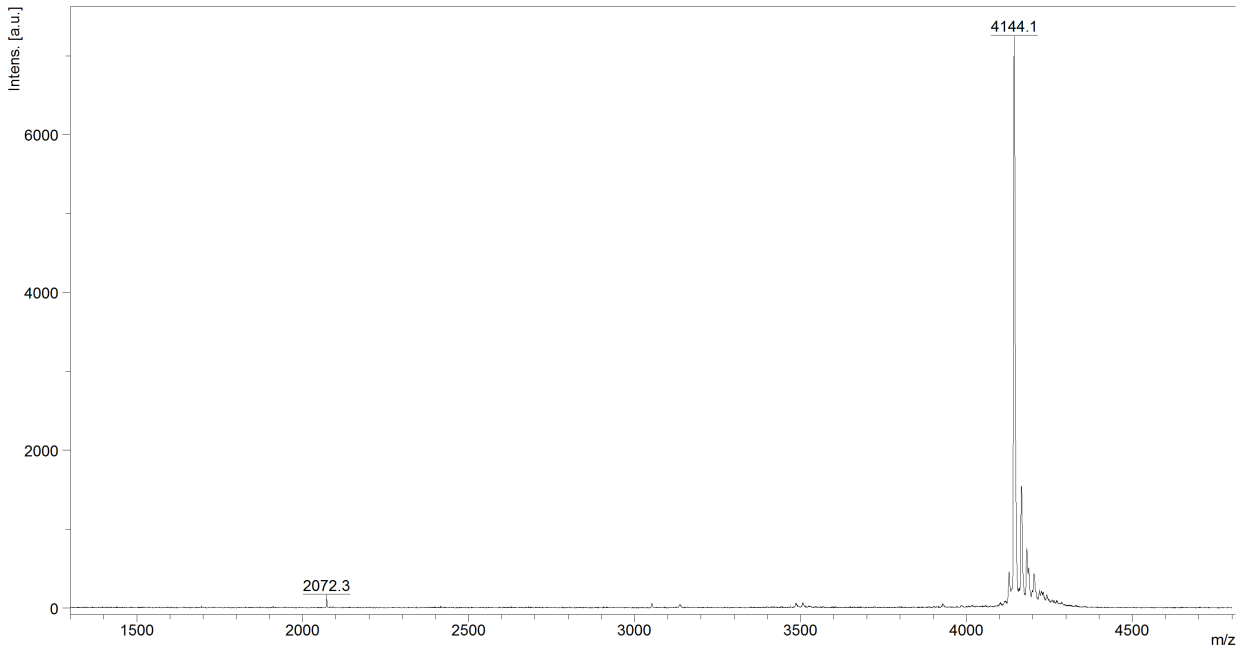

Figure S7. RSV HRC MALDI-TOF analysis

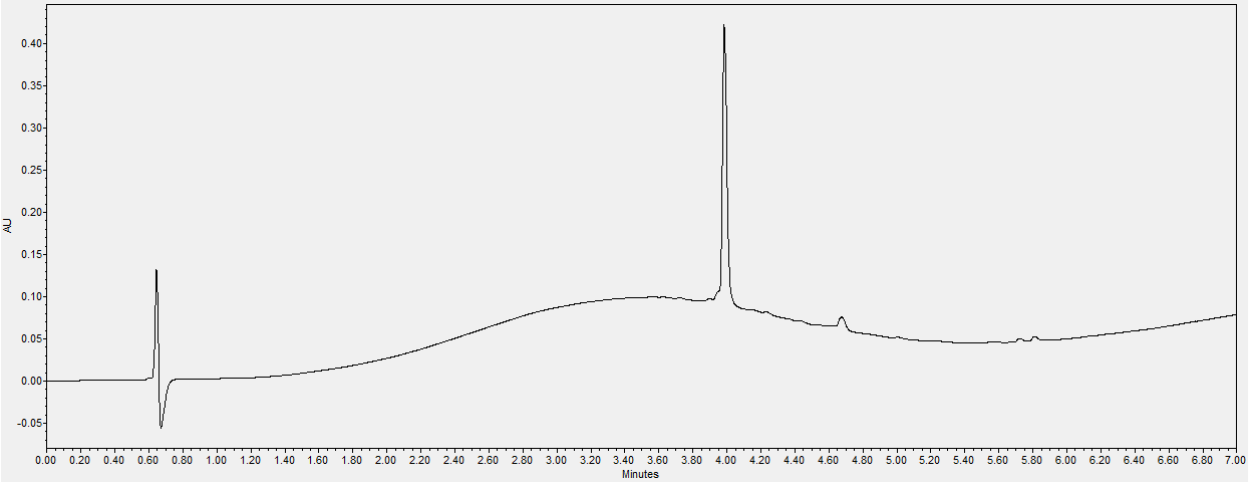

Figure S8. RSV HRC UPLC purity analysis, UPLC gradient from 10-95% MeCN/H_2O over 6 minutes (0.3 mL/min; column-Waters Acquity BEH C4 1.7 µm, 2.1 x 100 mm, purity >95%)

VI

Sequence: Ac-VALDPIDISIVLNKIKSDLEESKEWIRRSNQKLDSI-NH_2

Calculated monoisotopic [M+H]: 4206.3

Calculated monoisotopic [M+2H]: 2103.7

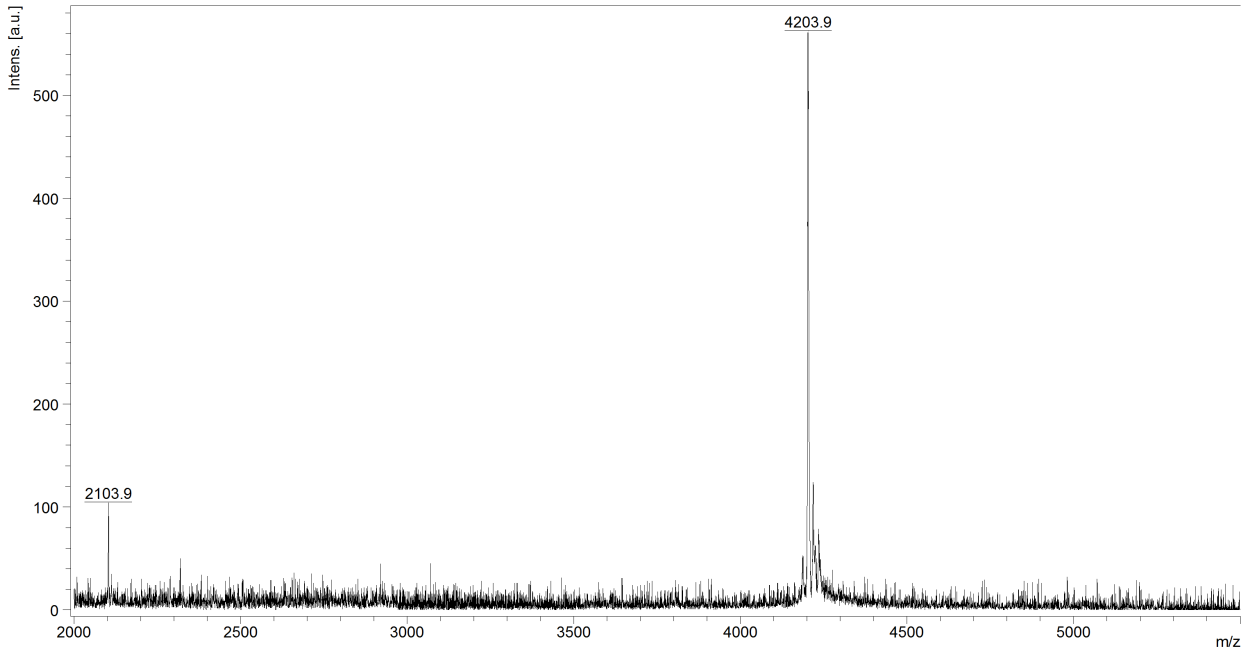

Figure S9. VI MALDI-TOF analysis

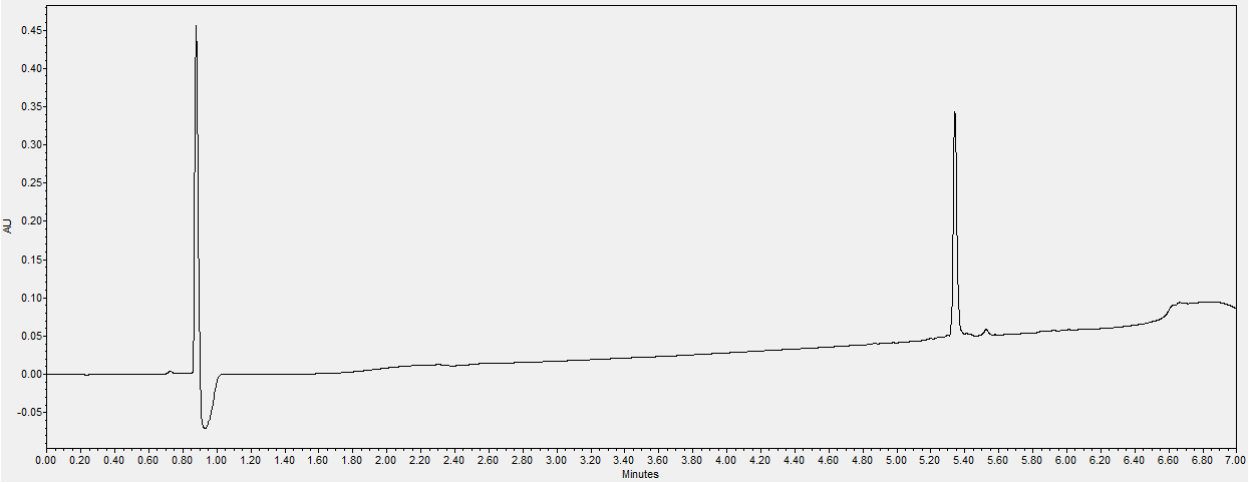

Figure S10. VI UPLC purity analysis, UPLC gradient from 10-95% MeCN/H_2O over 6 minutes (0.3 mL/min; column-Waters Acquity BEH C4 1.7 µm, 2.1 x 100 mm, purity >95%)

VIQKI

Sequence: Ac-VALDPIDISIVLNKIKSQLEESKEWIRRSNKILDSI-NH_2

Calculated monoisotopic [M+H]: 4204.4

Calculated monoisotopic [M+2H]: 2102.7

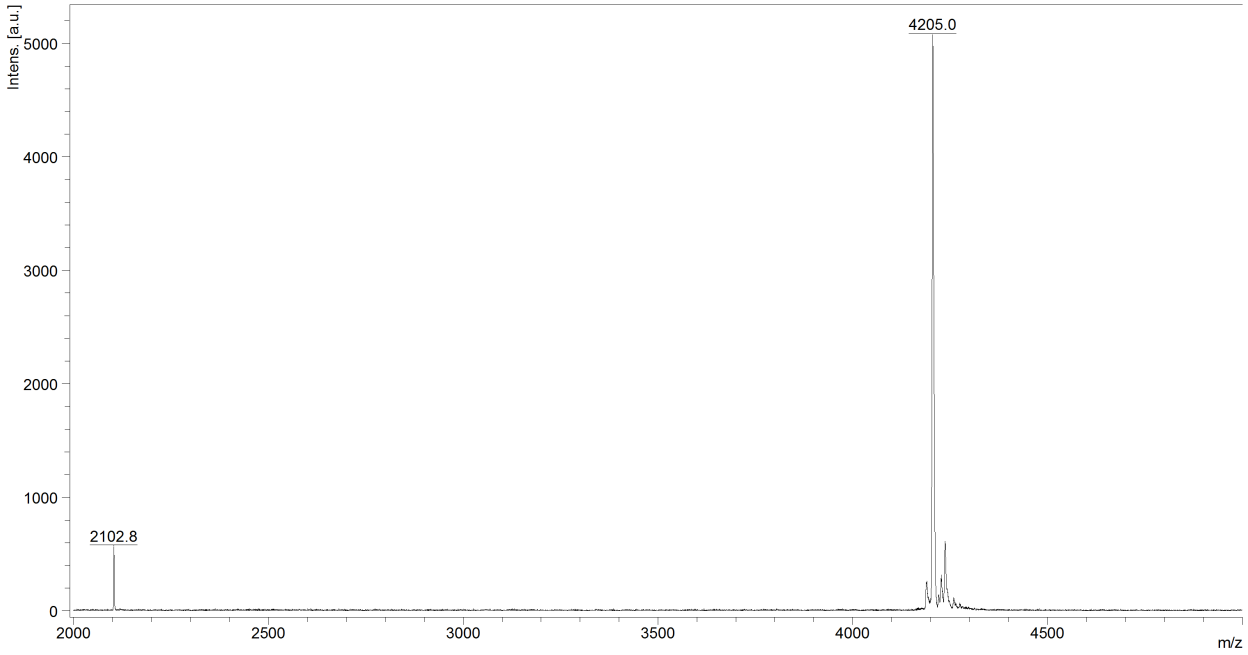

Figure S11. VIQKI MALDI-TOF analysis

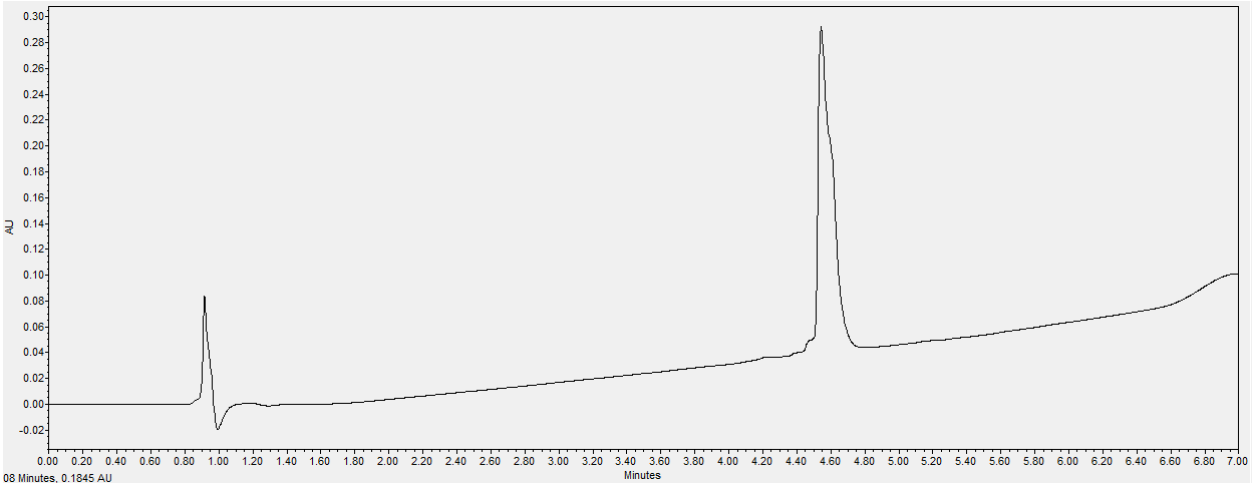

Figure S12. VIQKI UPLC purity analysis, UPLC gradient from 10-95% MeCN/H_2O over 6 minutes (0.3 mL/min; column-Waters Acquity BEH C4 1.7 μm, 2.1 x 100 mm, purity >95%)

VIQKI 452–484

Sequence: Ac-DPIDISIVLNKIKSQLEESKEWIRRSNKILDSI-NH_2

Calculated monoisotopic [M+H]: 3921.2

Calculated monoisotopic [M+2H]: 1961.1

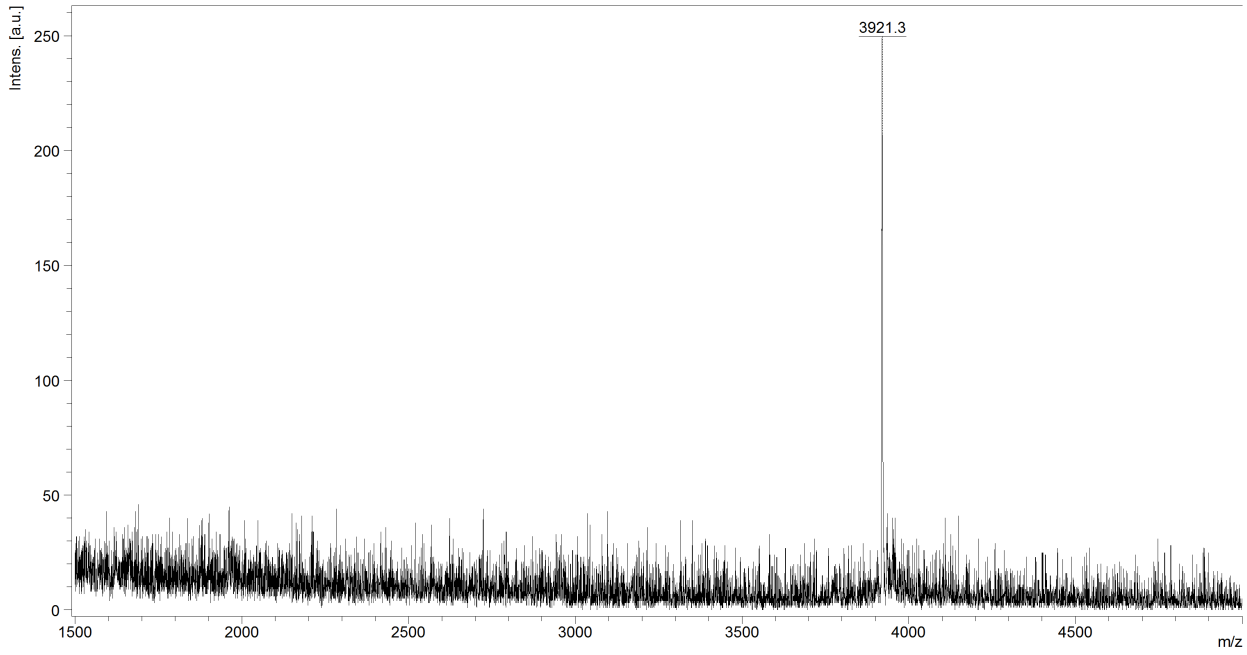

Figure S13. VIQKI 452–484 MALDI-TOF analysis

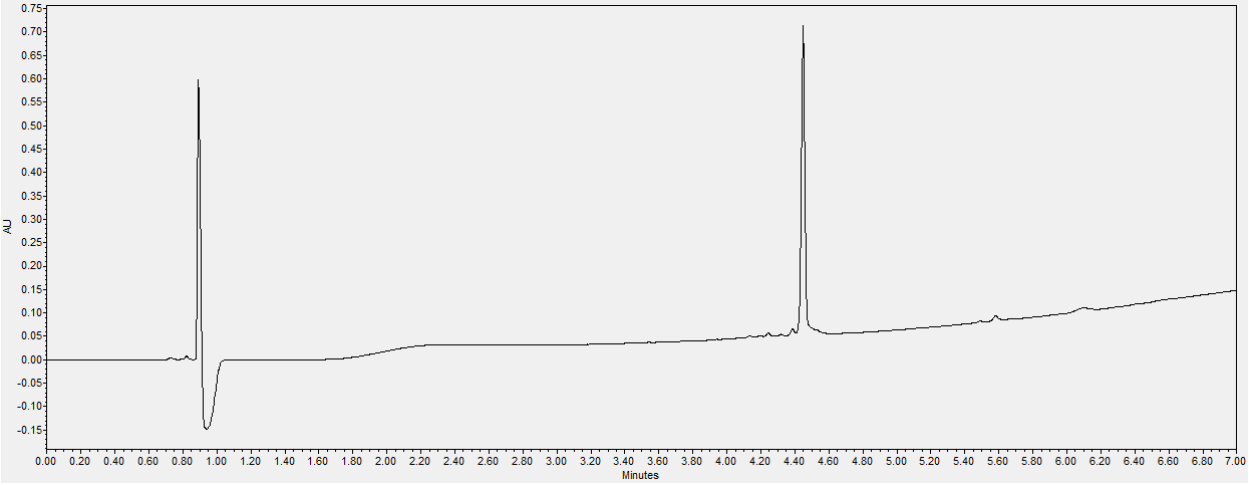

Figure S14. VIQKI 452–484 UPLC purity analysis, UPLC gradient from 10-95% MeCN/H_2O over 6 minutes (0.3 mL/min; column-Waters Acquity BEH C4 1.7 µm, 2.1 x 100 mm, purity >95%)

VIQKI 457–484

Sequence: Ac-SIVLNKIKSQLEESKEWIRRSNKILDSI-NH_2

Calculated monoisotopic [M+H]: 3367.9

Calculated monoisotopic [M+2H]: 1684.5

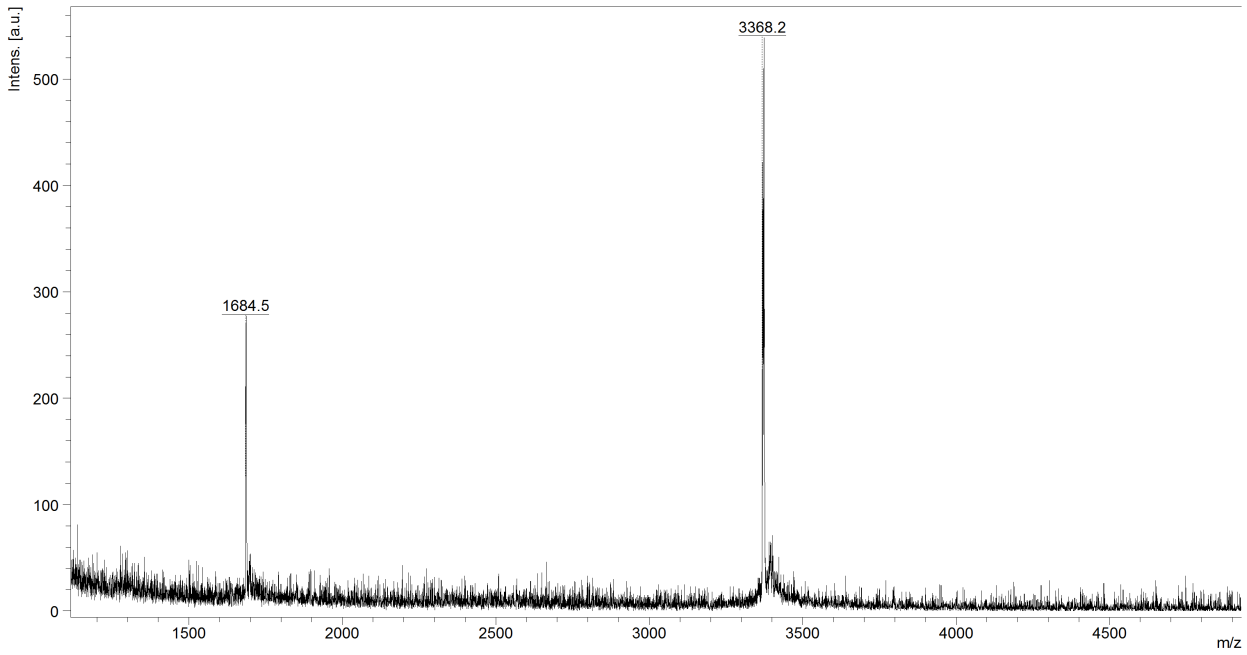

Figure S15. VIQKI 457–484 MALDI-TOF analysis

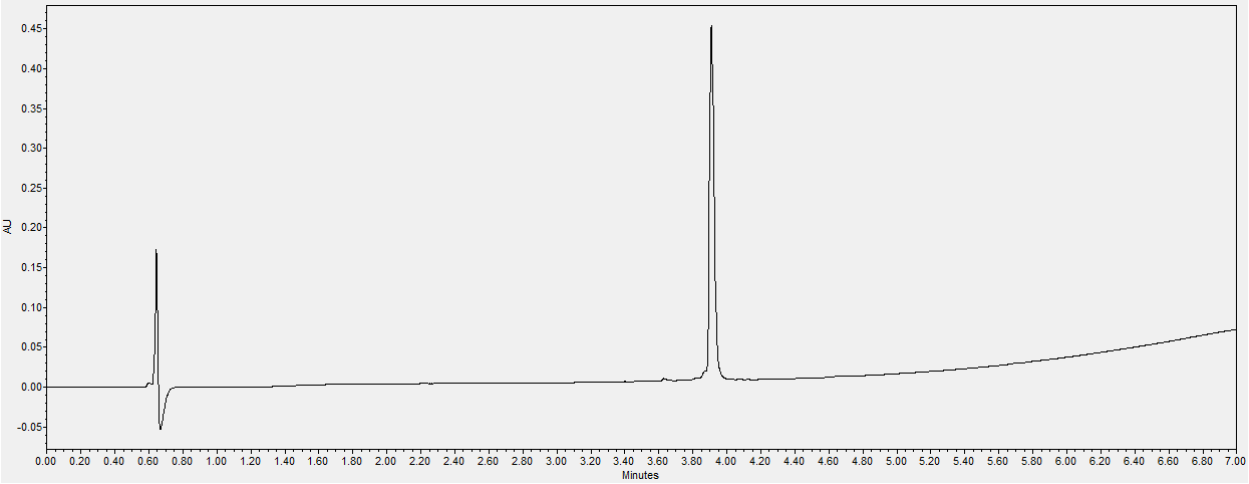

Figure S16. VIQKI 457–484 UPLC purity analysis, UPLC gradient from 10-95% MeCN/H_2O over 6 minutes (0.3 mL/min; column-Waters Acquity BEH C4 1.7 µm, 2.1 x 100 mm, purity >95%)

VIQKI V1A

Sequence: Ac-AALDPIDISIVLNKIKSQLEESKEWIRRSNKILDSI-NH_2

Calculated monoisotopic [M+H]: 4176.3

Calculated monoisotopic [M+2H]: 2088.7

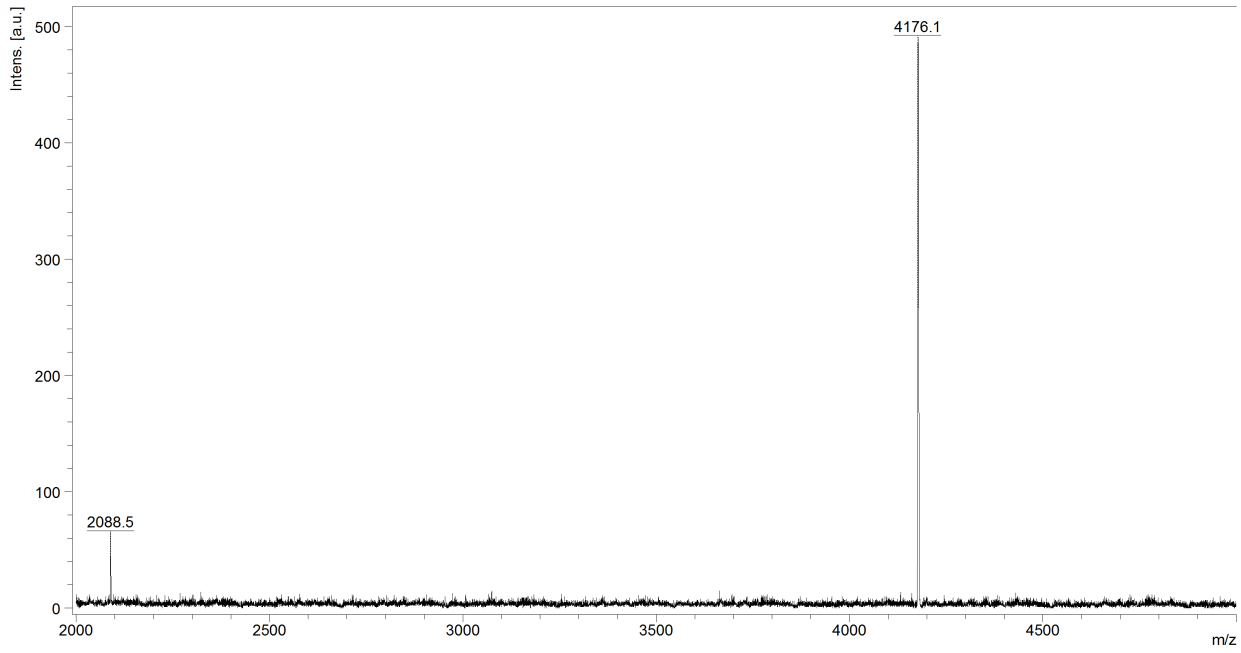

Figure S17. VIQKI V1A MALDI-TOF analysis

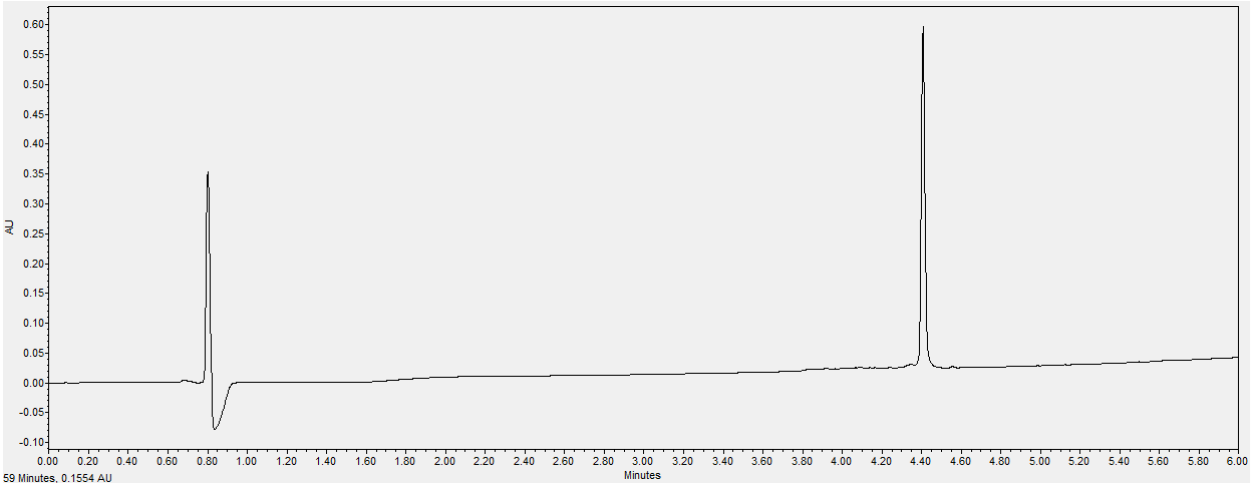

Figure S18. VIQKI V1A UPLC purity analysis, UPLC gradient from 10-95% MeCN/H_2O over 6 minutes (0.3 mL/min; column-Waters Acquity BEH C4 1.7 µm, 2.1 x 100 mm, purity >95%)

VIQKI L3A

Sequence: Ac-VAADPIDISIVLNKIKSQLEESKEWIRRSNKILDSI-NH_2

Calculated monoisotopic [M+H]: 4162.3

Calculated monoisotopic [M+2H]:2081.7

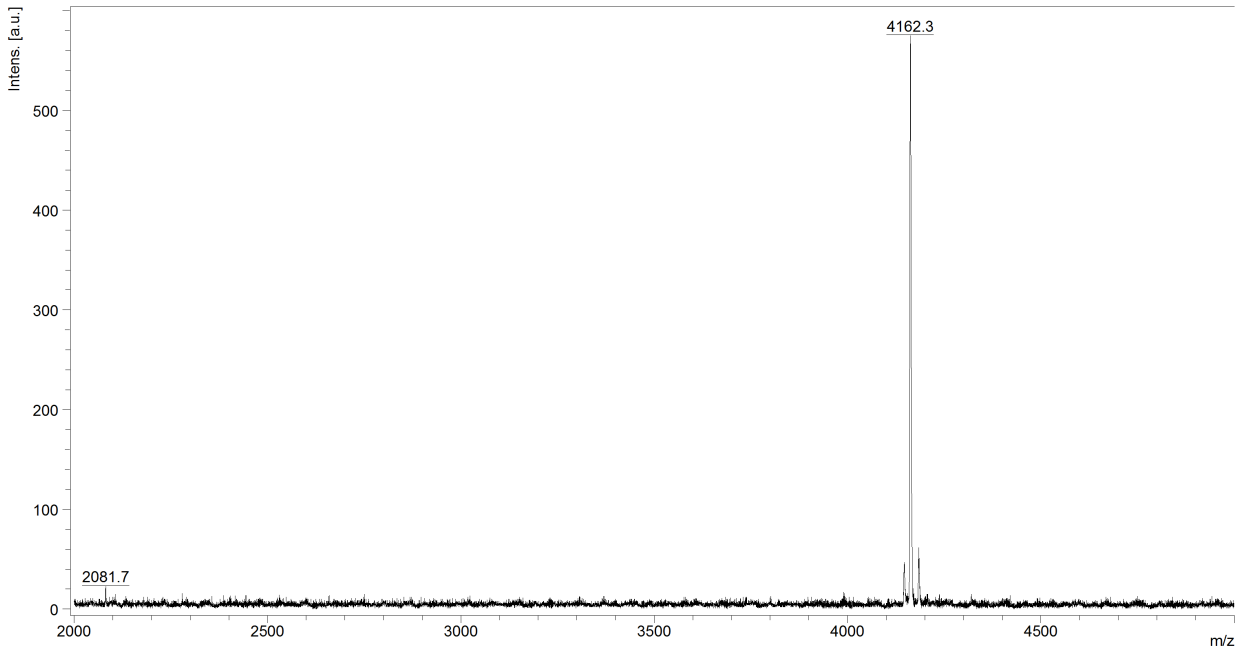

Figure S19. VIQKI L3A MALDI-TOF analysis

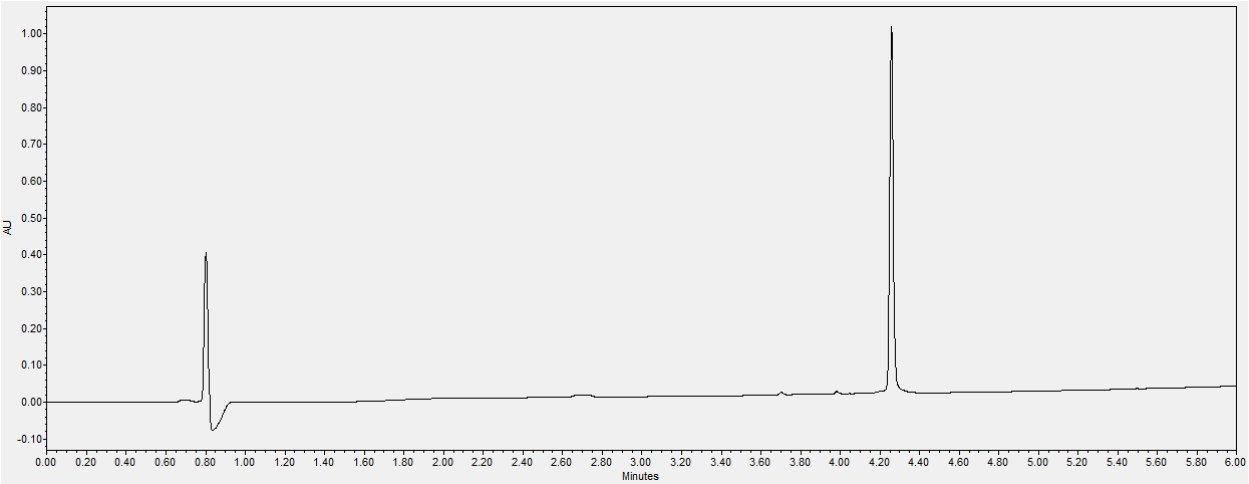

Figure S20. VIQKI L3A UPLC purity analysis, UPLC gradient from 10-95% MeCN/H_2O over 6 minutes (0.3 mL/min; column-Waters Acquity BEH C4 1.7 µm, 2.1 x 100 mm, purity >95%)

VIQKI D4A

Sequence: Ac-VALAPIDISIVLNKIKSQLEESKEWIRRSNKILDSI-NH_2

Calculated monoisotopic [M+H]: 4160.4

Calculated monoisotopic [M+2H]: 2080.7

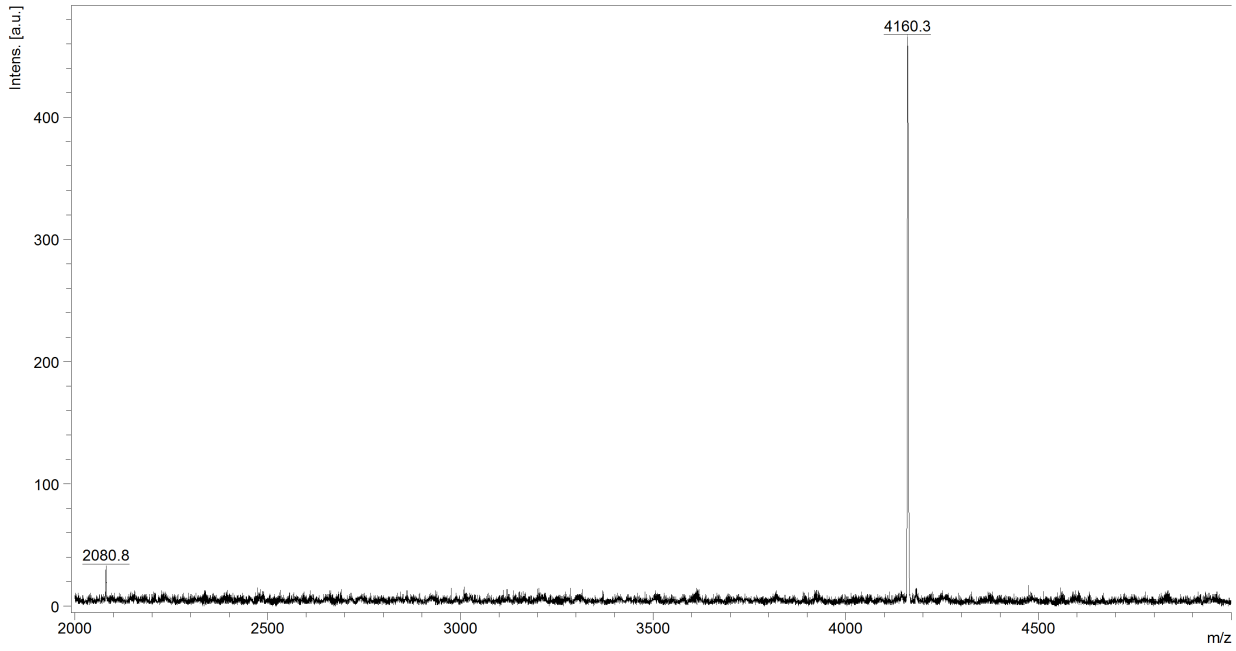

Figure S21. VIQKI D4A MALDI-TOF analysis

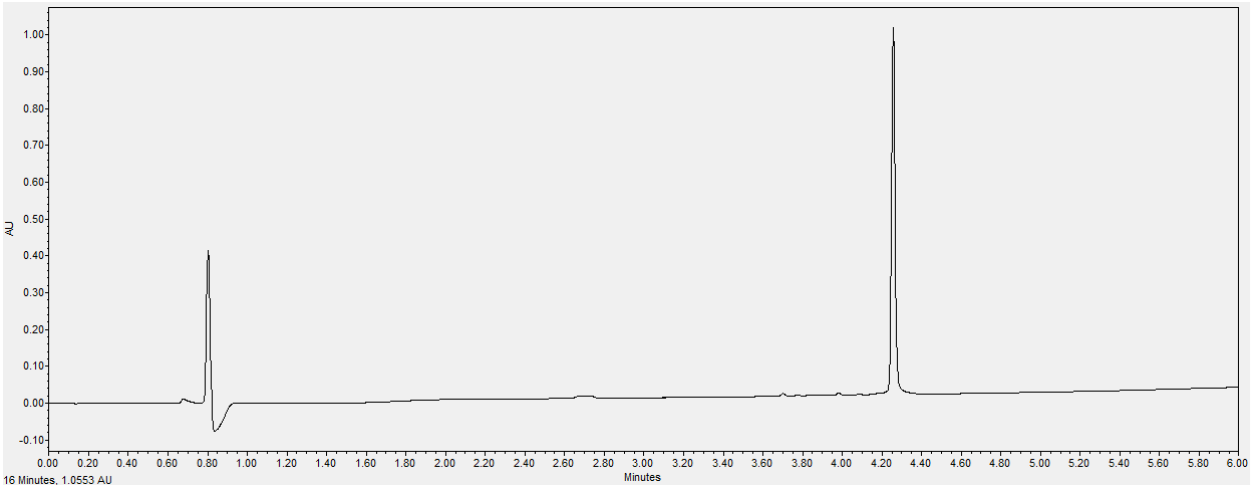

Figure S22. VIQKI D4A UPLC purity analysis, UPLC gradient from 10-95% MeCN/H_2O over 6 minutes (0.3 mL/min; column-Waters Acquity BEH C4 1.7 µm, 2.1 x 100 mm, purity >95%)

VIQKI P5A

Sequence: Ac-VALDAIDISIVLNKIKSQLEESKEWIRRSNKILDSI-NH_2

Calculated monoisotopic [M+H]: 4178.4

Calculated monoisotopic [M+2H]: 2089.7

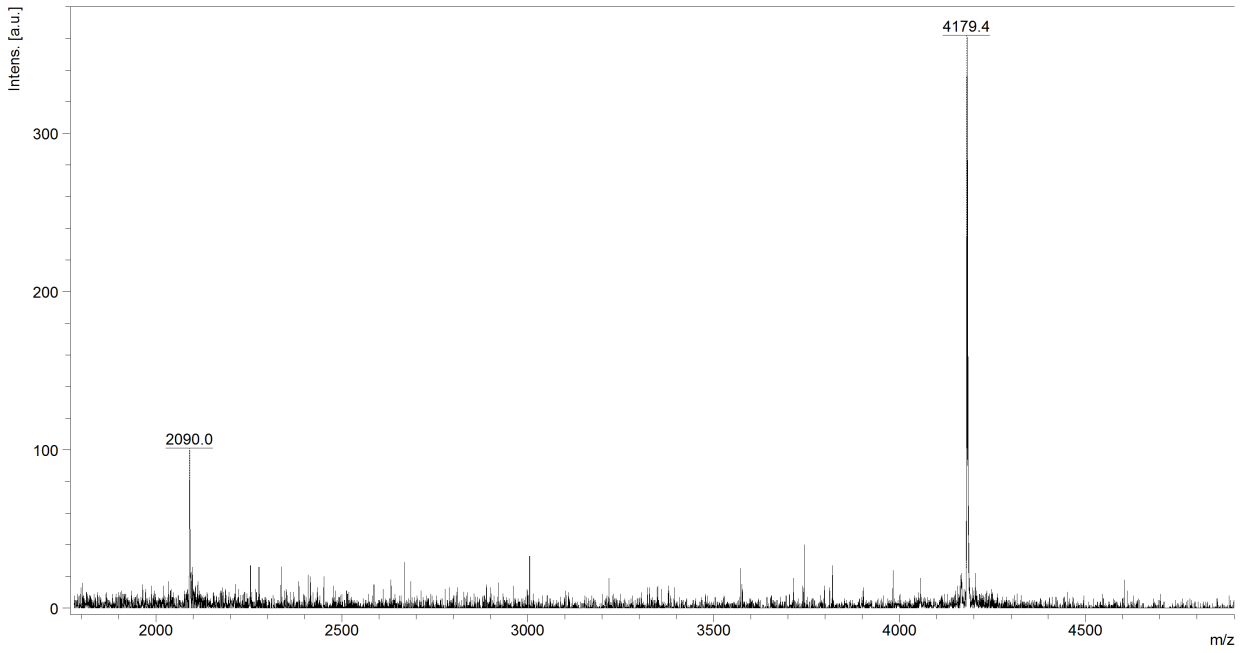

Figure S23. VIQKI P5A MALDI-TOF analysis

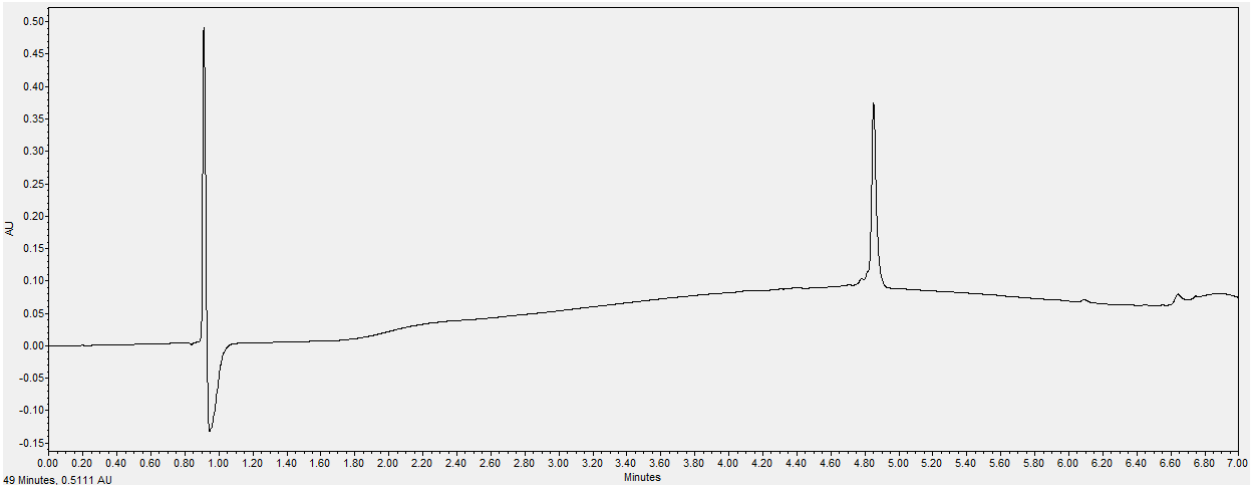

Figure S24. VIQKI P5A UPLC purity analysis, UPLC gradient from 10-95% MeCN/H_2O over 6 minutes (0.3 mL/min; column-Waters Acquity BEH C4 1.7 µm, 2.1 x 100 mm, purity >95%)

VIQKI I6A

Sequence: Ac-VALDPADISIVLNKIKSQLEESKEWIRRSNKILDSI-NH_2

Calculated monoisotopic [M+H]: 4162.3

Calculated monoisotopic [M+2H]: 2081.7

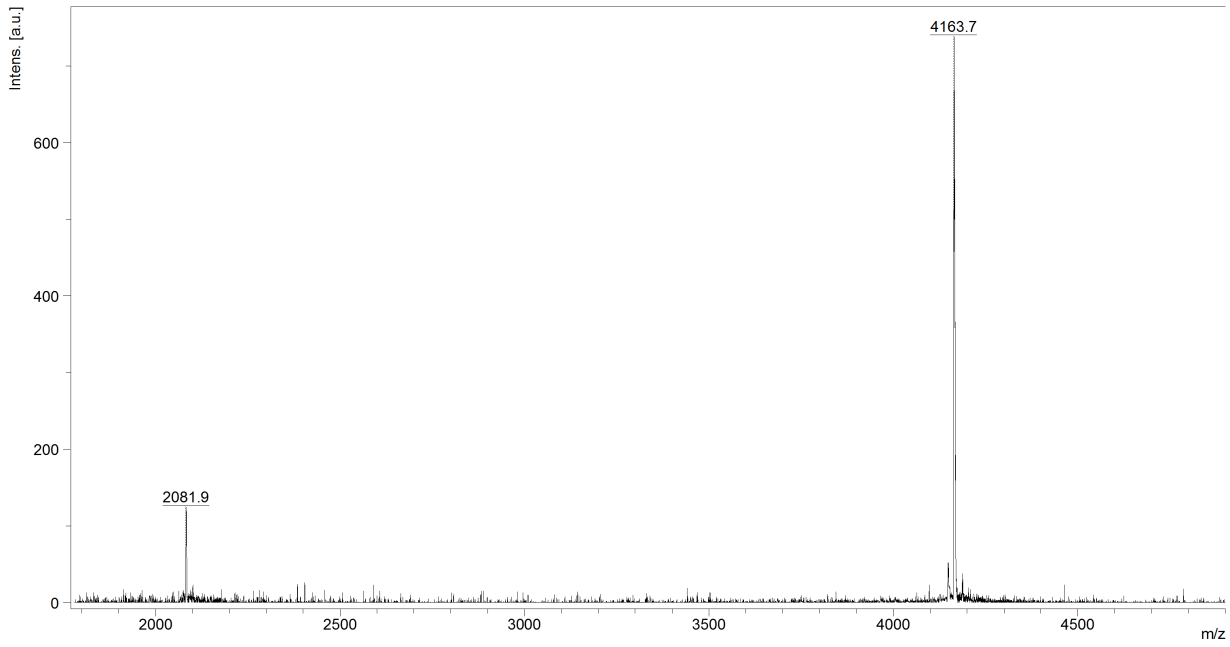

Figure S25. VIQKI I6A MALDI-TOF analysis

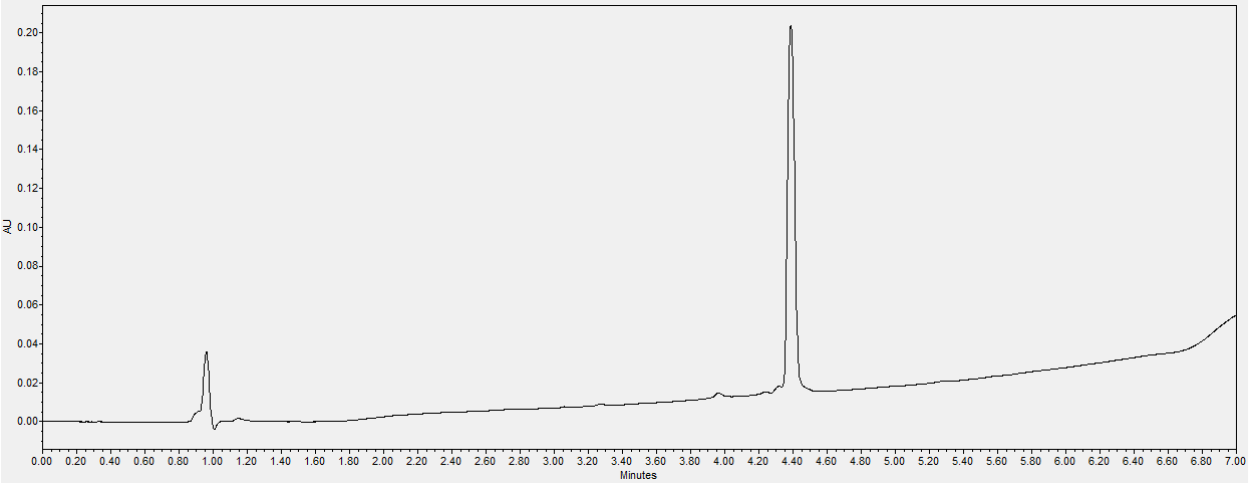

Figure S26. VIQKI I6A UPLC purity analysis, UPLC gradient from 10-95% MeCN/H_2O over 6 minutes (0.3 mL/min; column-Waters Acquity BEH C4 1.7 μm, 2.1 x 100 mm, purity >95%)

VIQKI D7A

Sequence: Ac-VALDPIAISIVLNKIKSQLEESKEWIRRSNKILDSI-NH_2

Calculated monoisotopic [M+H]: 4161.4

Calculated monoisotopic [M+2H]: 2080.7

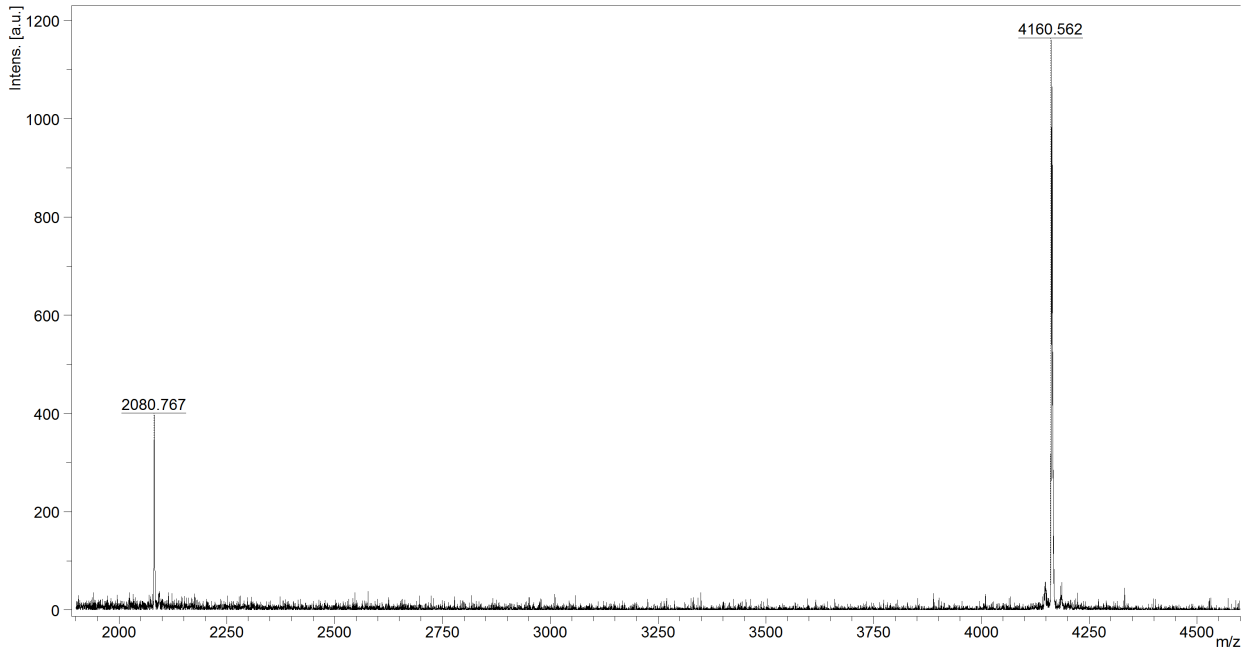

Figure S27. VIQKI D7A MALDI-TOF analysis

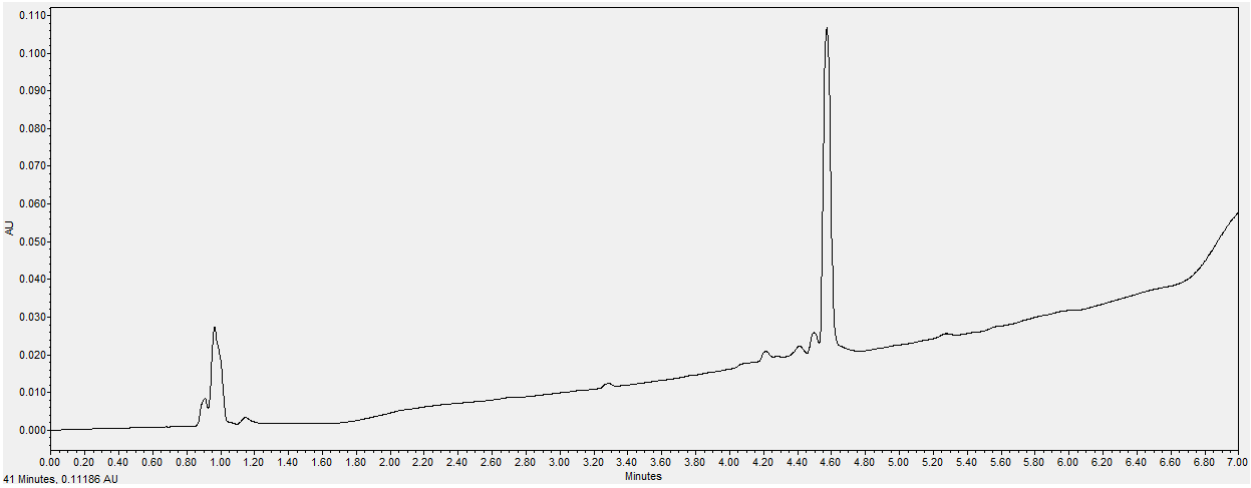

Figure S28. VIQKI D7A UPLC purity analysis, UPLC gradient from 10-95% MeCN/H_2O over 6 minutes (0.3 mL/min; column-Waters Acquity BEH C4 1.7 µm, 2.1 x 100 mm, purity >95%)

VIQKI I8A

Sequence: Ac-VALDPIDASIVLNKIKSQLEESKEWIRRSNKILDSI-NH_2

Calculated monoisotopic [M+H]: 4162.3

Calculated monoisotopic [M+2H]: 2081.7

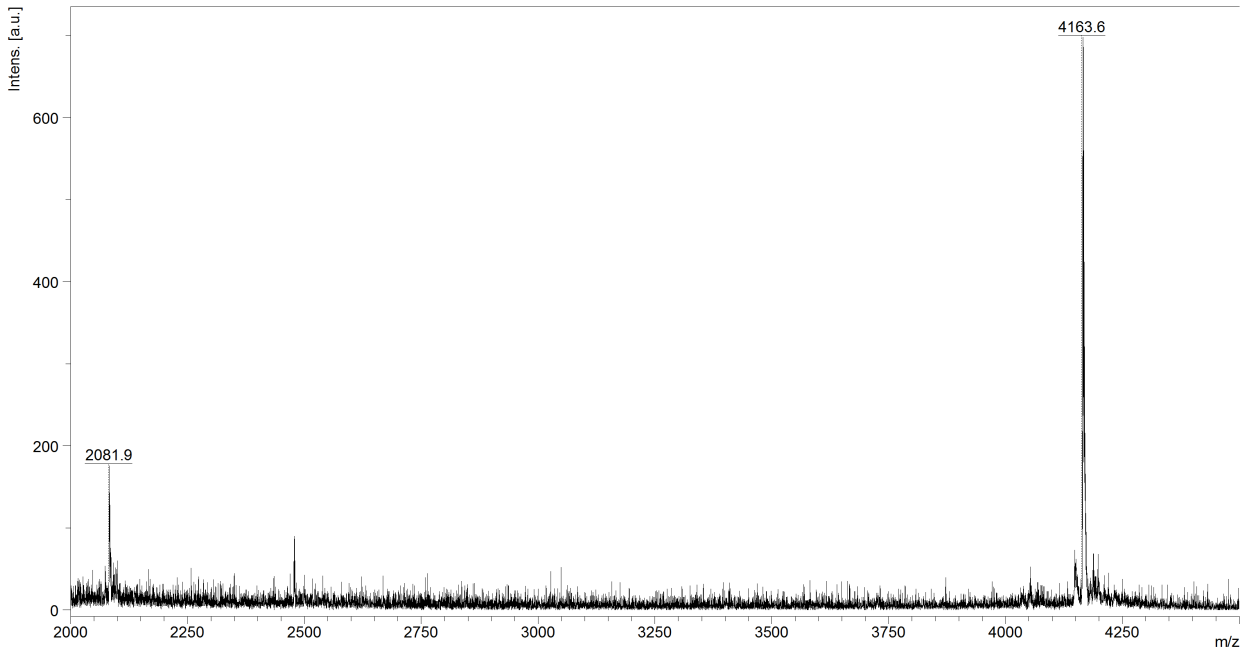

Figure S29. VIQKI I8A MALDI-TOF analysis

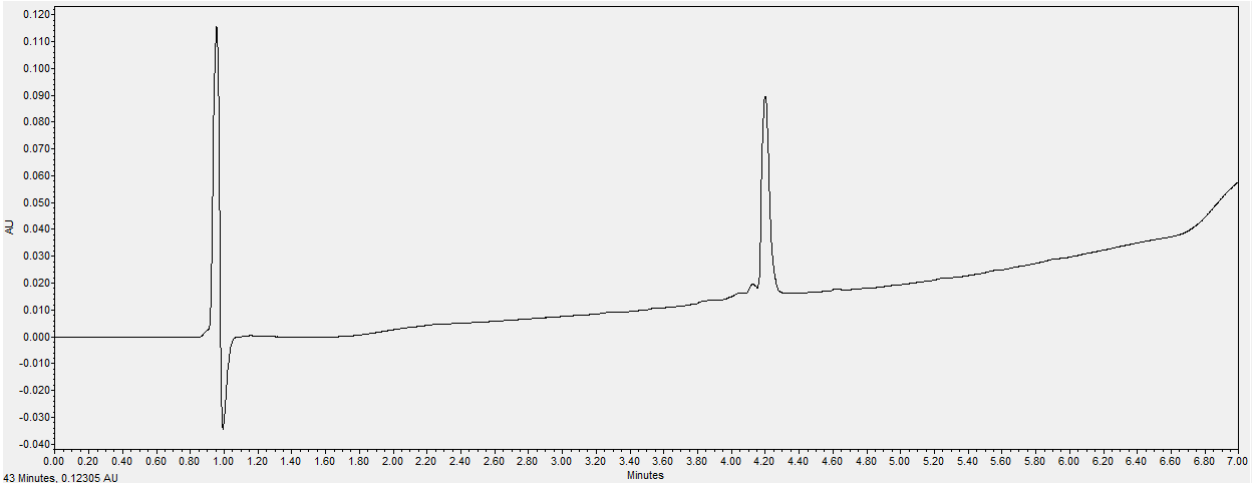

Figure S30. VIQKI I8A UPLC purity analysis, UPLC gradient from 10-95% MeCN/H_2O over 6 minutes (0.3 mL/min; column-Waters Acquity BEH C4 1.7 µm, 2.1 x 100 mm, purity >95%)

VIQKI S9A

Sequence: Ac-VALDPIDIAIVLNKIKSQLEESKEWIRRSNKILDSI-NH_2

Calculated monoisotopic [M+H]: 4188.4

Calculated monoisotopic [M+2H]: 2094.7

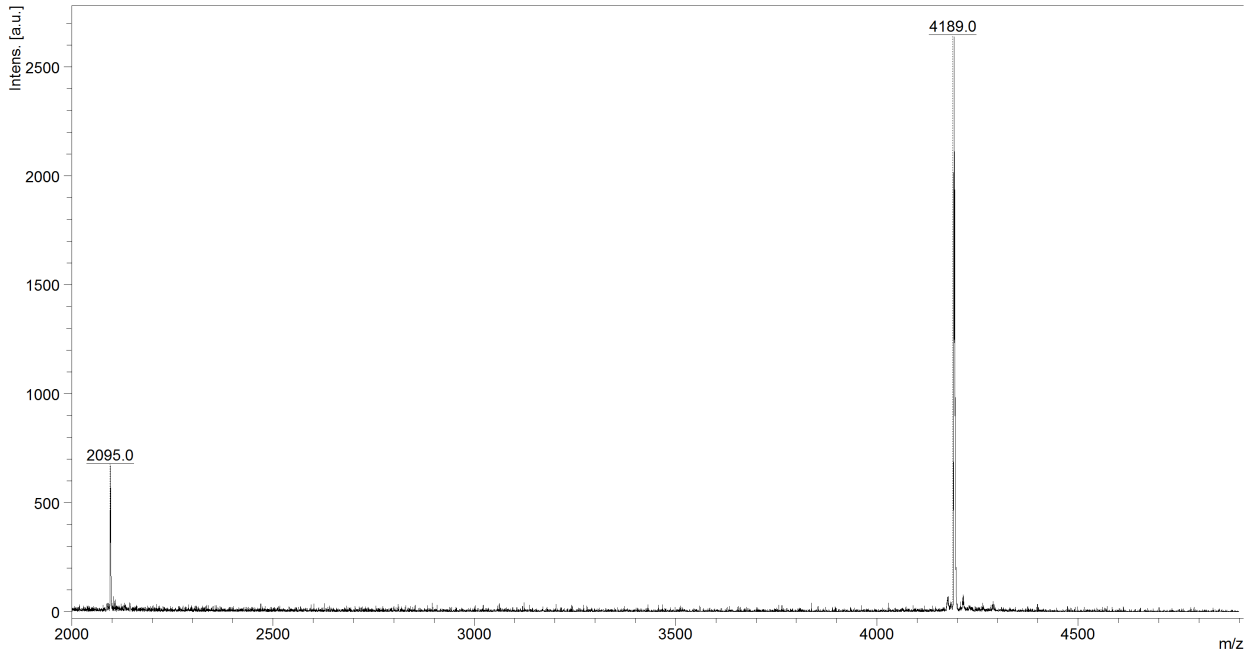

Figure S31. VIQKI S9A MALDI-TOF analysis

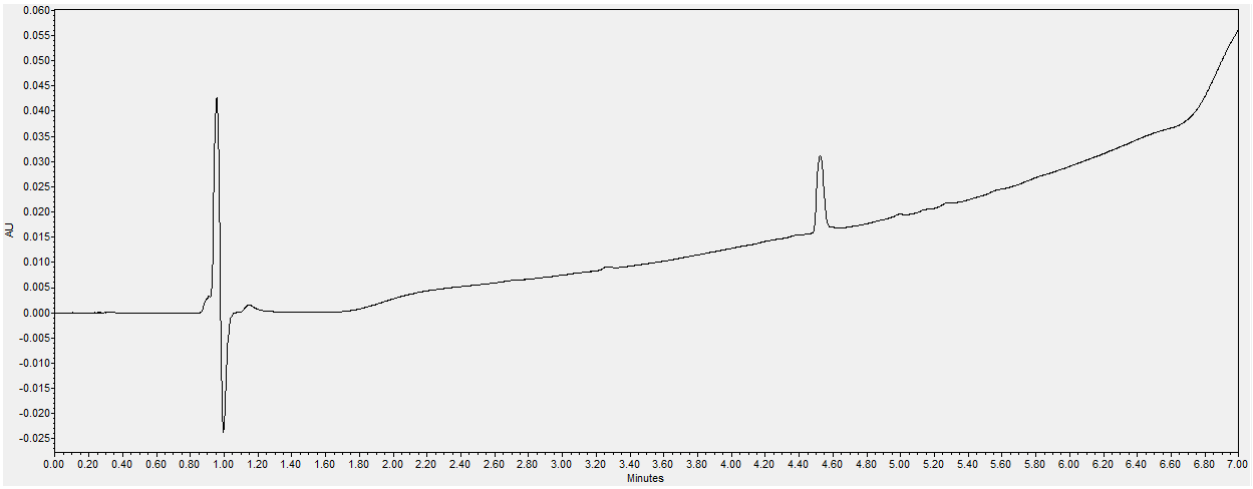

Figure S32. VIQKI S9A UPLC purity analysis, UPLC gradient from 10-95% MeCN/H_2O over 6 minutes (0.3 mL/min; column-Waters Acquity BEH C4 1.7 µm, 2.1 x 100 mm, purity >95%)

Circular Dichroism Spectroscopy

All circular dichroism (CD) spectroscopy experiments were performed on an Aviv Biomedical model 420 CD spectrometer. Samples were prepared in 1 mm quartz strain-free cuvettes (Helma) using 50 μM peptide in phosphate buffered saline (PBS). Wavelength scans were collected from 260 nm to 200 nm with a 1 nm bandwidth and 10 second averaging time. The CD spectrometer was calibrated with a 1 mg/mL solution of camphor sulfonic acid (CSA) in water. For thermal denaturation experiments, ellipticity was measured at 222 nm as temperature was raised from 5–98 °C in 3-degree increments with a 5-minute equilibration time and a 10-second averaging time for each measurement.

Comparing Individual HRN and HRC Peptides with their Binary Mixtures via CD

We used CD measurements (wavelength scans) to determine whether specific pairs of HRN and HRC peptides could co-assemble in PBS. Co-assembly is known to enhance α-helix formation, which can be detected by minima at 208 and 222 nm in the CD spectrum. In each case, we measured the CD spectrum of each peptide in isolation (50 uM peptide) and the CD spectrum of a 1:1 mixture of the two peptides (50 uM each). We compared the CD signal (in mdeg) of the 1:1 mixture (red trace) with the mathematical sum of the spectra of the individual peptides (gray trace). If the intensities at 208 and 222 nm for the mixture are significantly greater than the intensities at the same wavelengths for the mathematical sum of the individual peptides, then we conclude that co-assembly has occurred.

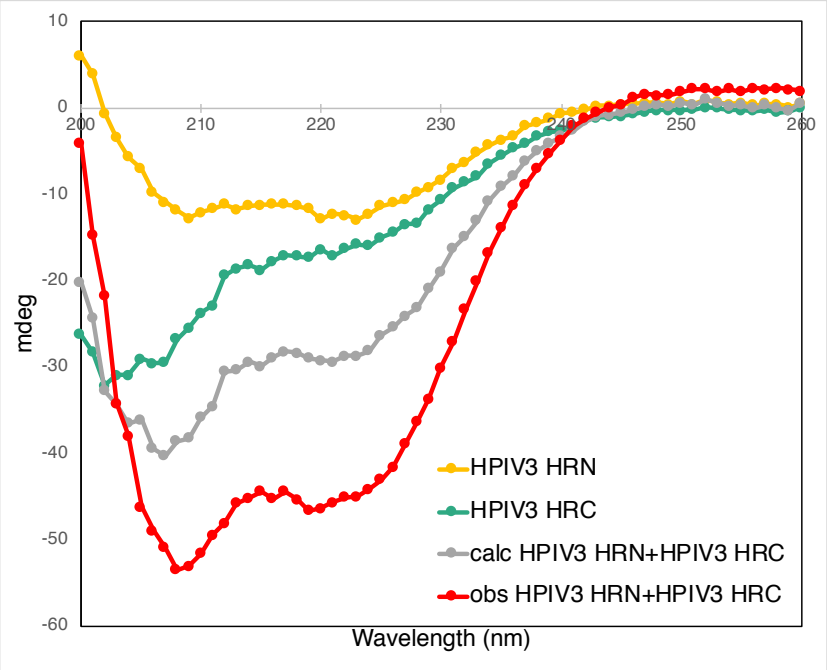

Figure S33 Wavelength scan of HPIV3 HRN (orange), HPIV3 HRC (green), mathematical sum of individual HRN and HRC spectra (gray), and 1:1 mixture of HPIV3 HRN+HPIV3 HRC (red) peptides

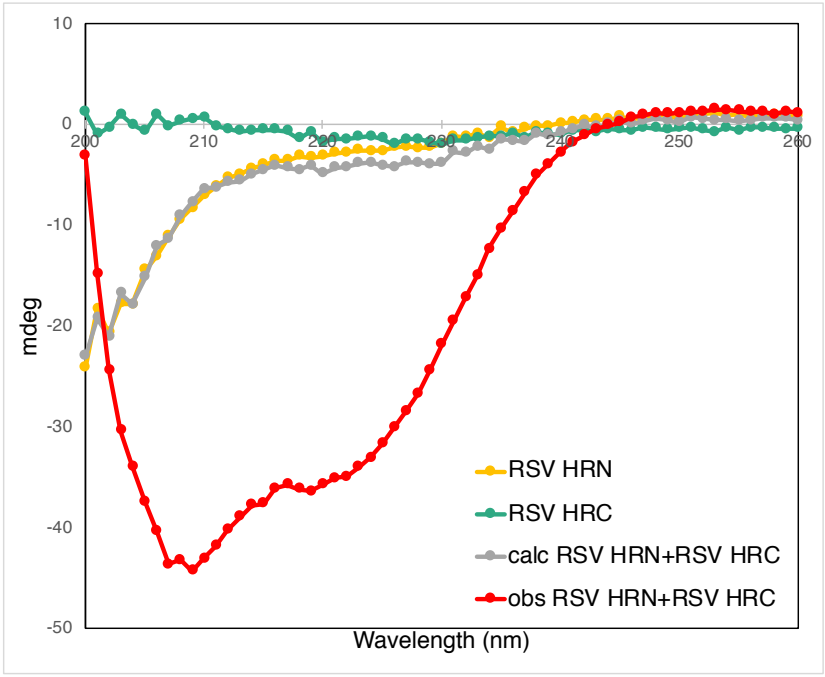

Figure S34 Wavelength scan of RSV HRN (orange), RSV HRC (green), mathematical sum of individual HRN and HRC spectra (gray), and 1:1 mixture of RSV HRN+RSV HRC (red) peptides

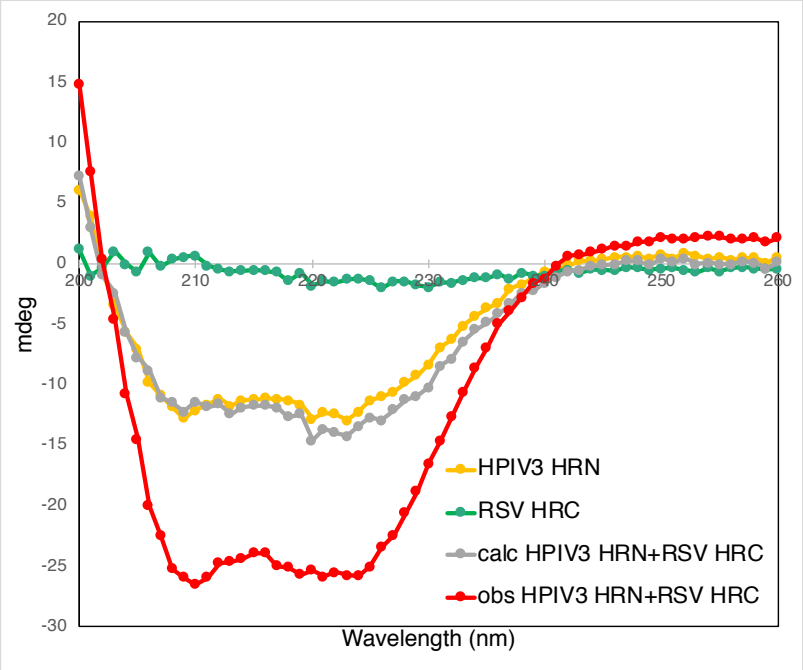

Figure S35 Wavelength scan of HPIV3 HRN (orange), RSV HRC (green), mathematical sum of individual HRN and HRC spectra (gray), and 1:1 mixture of HPIV3 HRN+RSV HRC (red) peptides

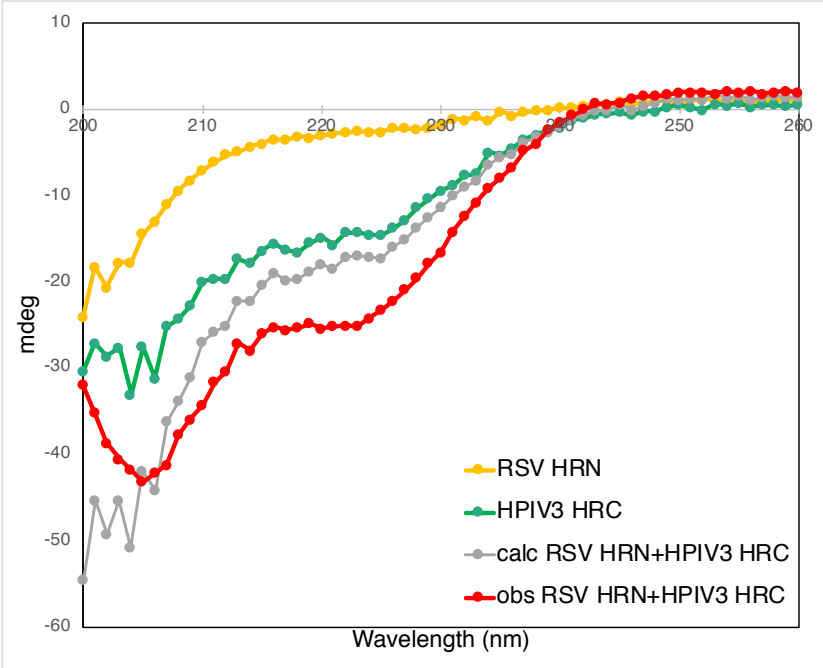

Figure S36 Wavelength scan of RSV HRN (orange), HPIV3 HRC (green), mathematical sum of individual HRN and HRC spectra (gray), and 1:1 mixture of RSV HRN+HPIV3 HRC (red) peptides

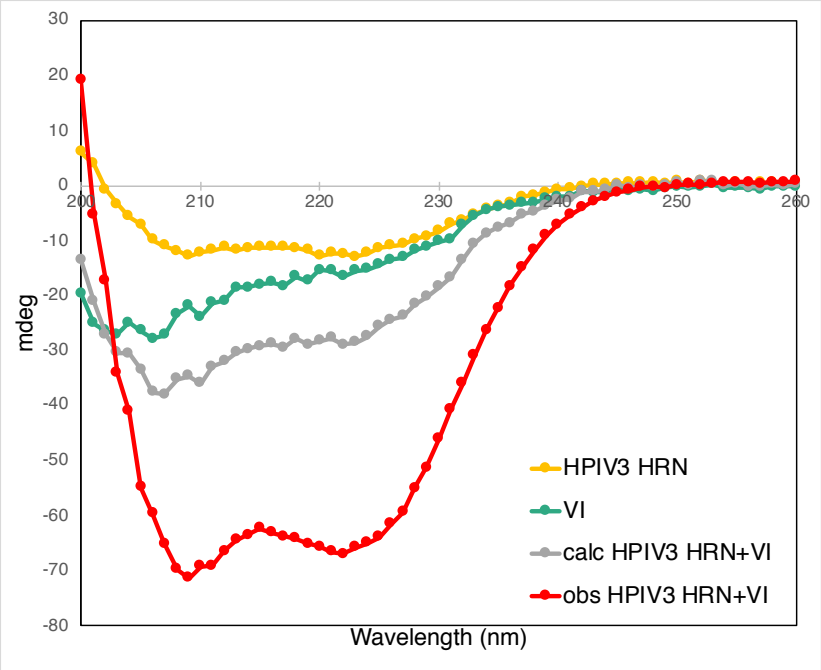

Figure S37 Wavelength scan of HPIV3 HRN (orange), VI (green), mathematical sum of individual HRN and HRC spectra (gray), and 1:1 mixture of HPIV3 HRN+VI (red) peptides

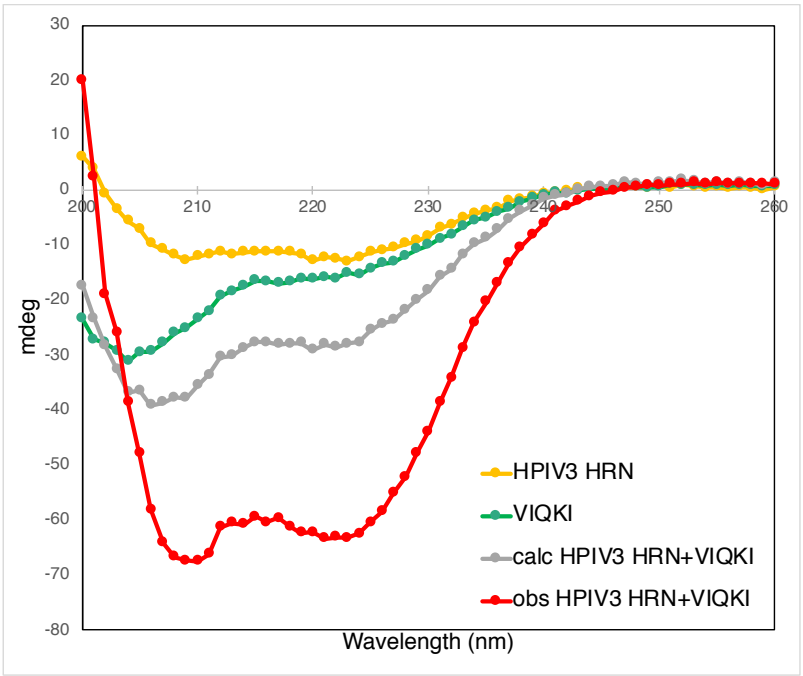

Figure S38 Wavelength scan of HPIV3 HRN (orange), VIQKI (green), mathematical sum of individual HRN and HRC spectra (gray), and 1:1 mixture of HPIV3 HRN+VIQKI (red) peptides

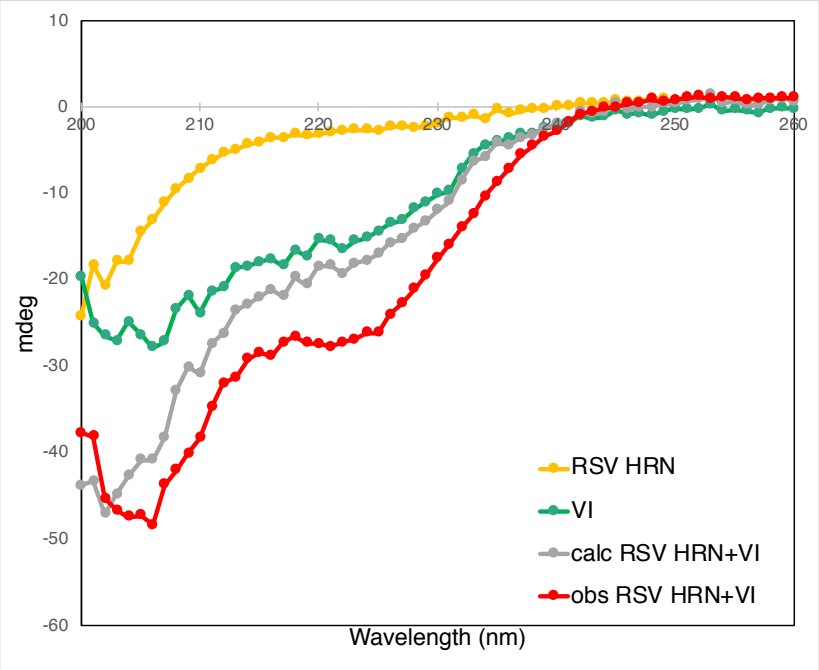

Figure S39 Wavelength scan of RSV HRN (orange), VI (green), mathematical sum of individual HRN and HRC spectra (gray), and 1:1 mixture of RSV HRN+VI (red) peptides

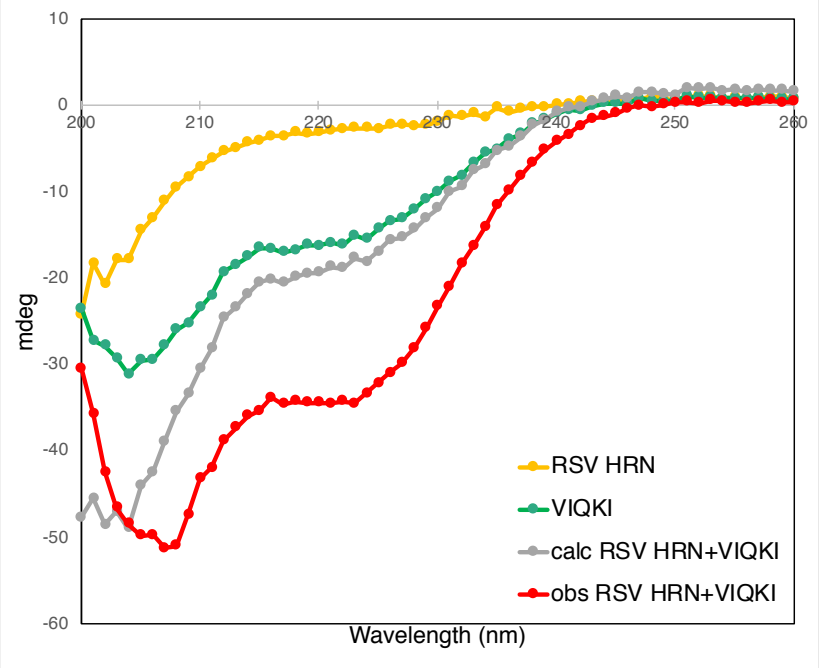

Figure S40 Wavelength scan of RSV HRN (orange), VIQKI (green), mathematical sum of individual HRN and HRC spectra (gray), and 1:1 mixture of RSV HRN+VIQKI (red) peptides

Comparing Peptide Mixtures Involving the HPIV3 HRN Peptide or the RSV HRN Peptide

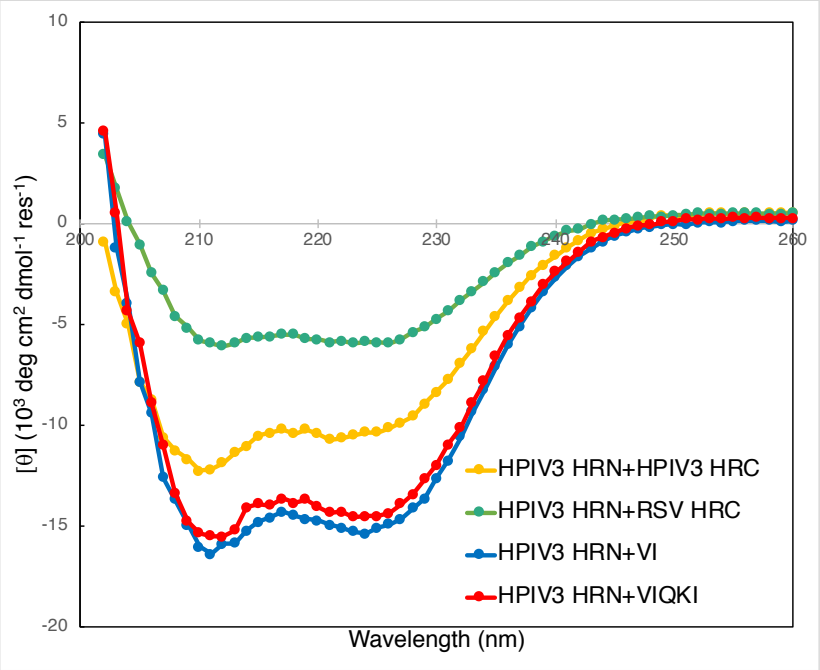

Figure S41 Wavelength scans of 1:1 mixtures of HPIV3 HRN with HPIV3 HRC (orange), RSV HRC (green), VI (gray), or VIQKI (red)

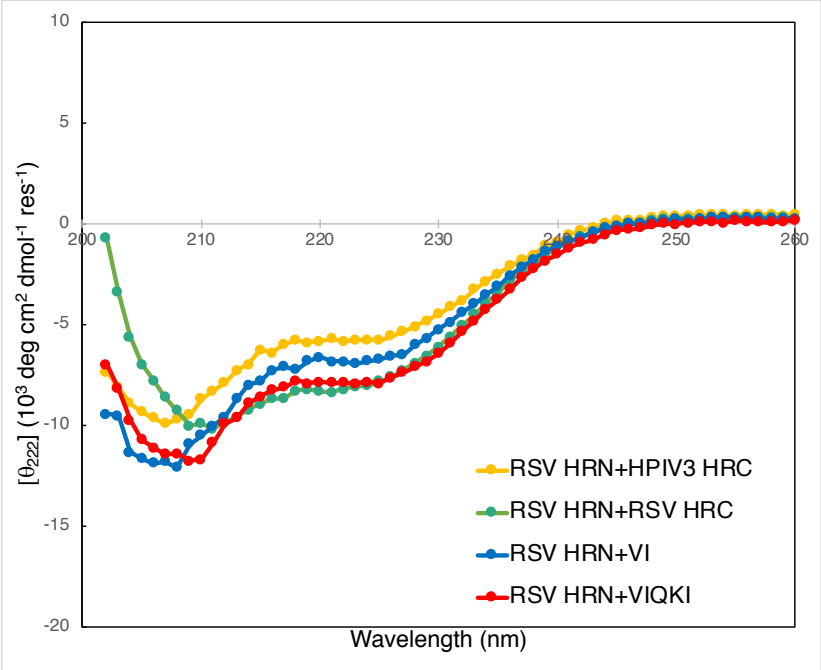

Figure S42 Wavelength scans of 1:1 mixtures of RSV HRN with HPIV3 HRC (orange), RSV HRC (green), VI (gray), or VIQKI (red)

Thermal Denaturation Assays for Specific HRN+HRC Pairs

In each thermal denaturation experiment, ellipticity of a 1:1 mixture of two peptides (50 μM each in PBS) was measured at 222 nm as temperature was raised from 5–98 °C in 3-degree increments with a 5-minute equilibration time and a 10-second averaging time for each measurement.

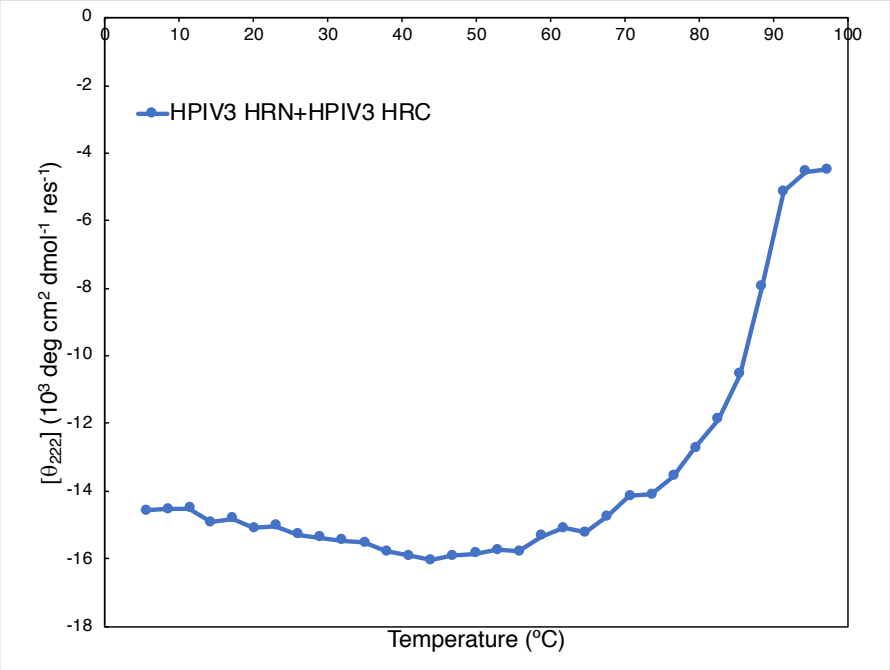

Figure S43 Thermal denaturation of 1:1 mixture of HPIV3 HRN+HPIV3 HRC

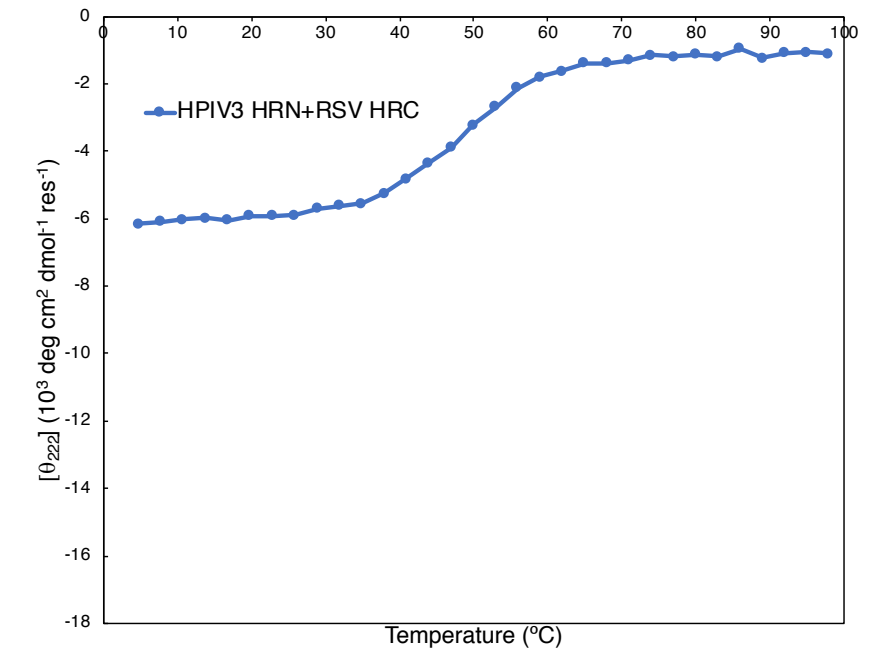

Figure S44 Thermal denaturation of 1:1 mixture of HPIV3 HRN+RSV HRC

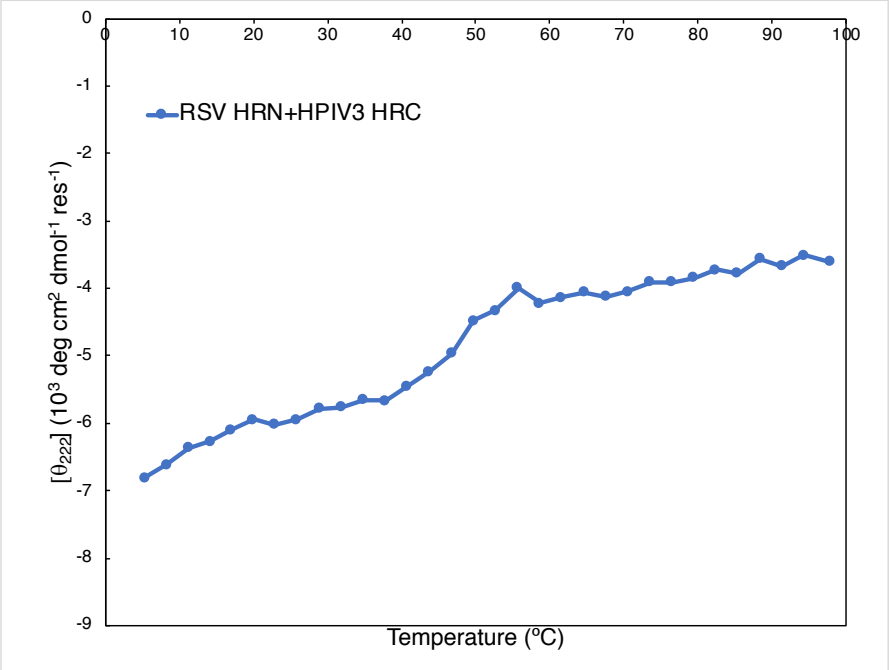

Figure S45 Thermal denaturation of 1:1 mixture of RSV HRN+HPIV3 HRC

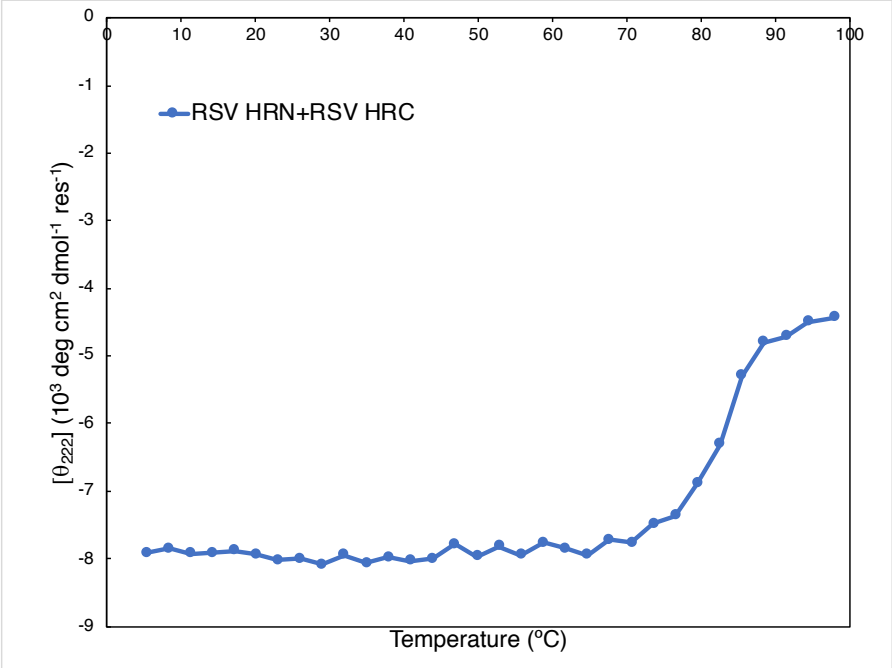

Figure S46 Thermal denaturation of 1:1 mixture of RSV HRN+RSV HRC

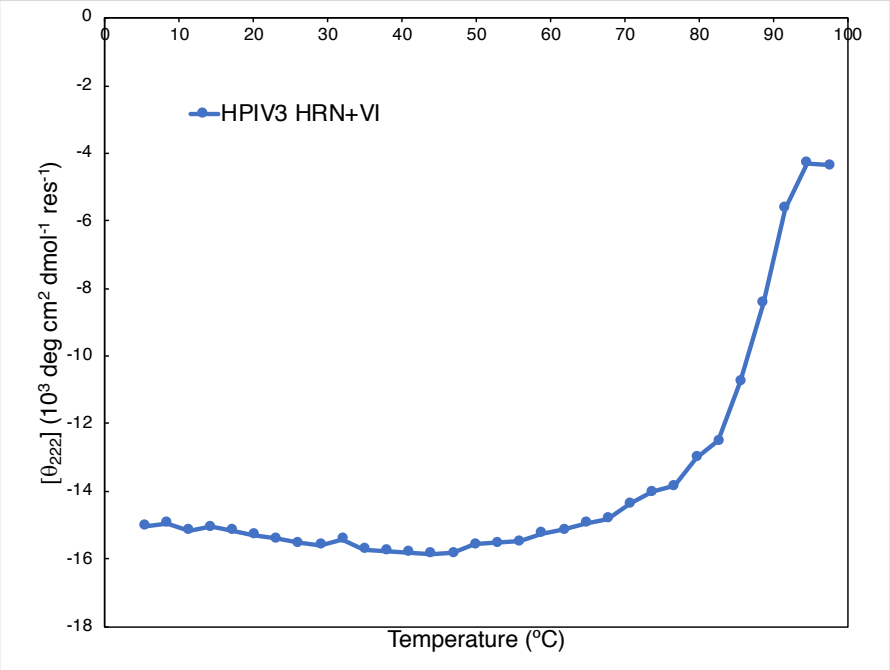

Figure S47 Thermal denaturation of 1:1 mixture of HPIV3 HRN+VI

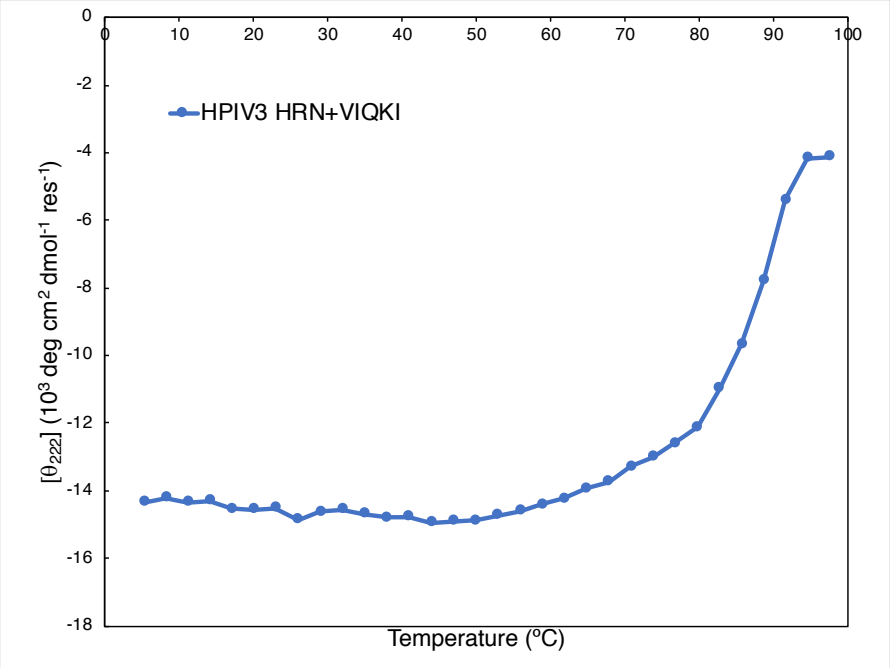

Figure S48 Thermal denaturation of 1:1 mixture of HPIV3 HRN+VIQKI

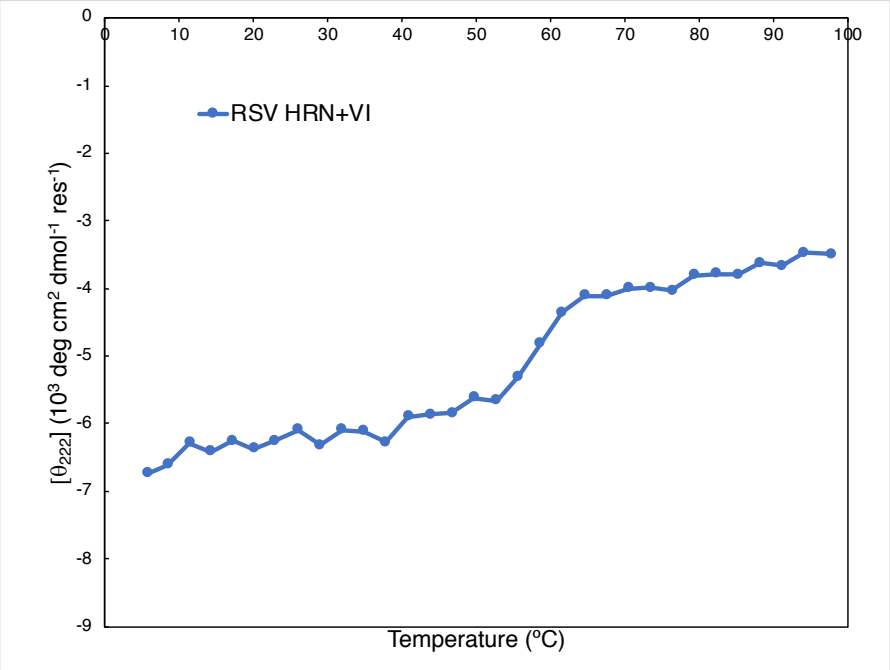

Figure S49 Thermal denaturation of 1:1 mixture of RSV HRN+VI

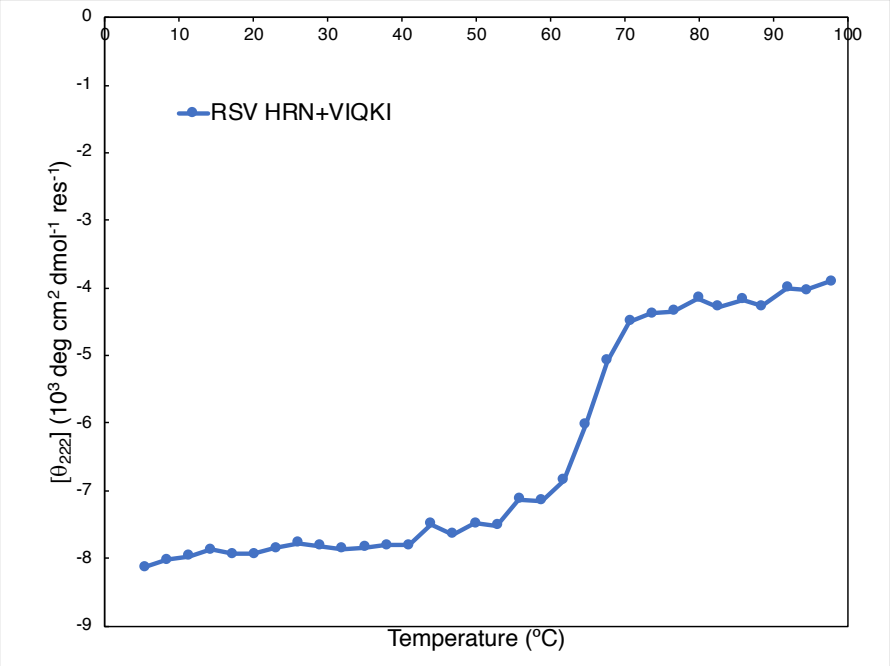

Figure S50 Thermal denaturation of 1:1 mixture of RSV HRN+VIQKI

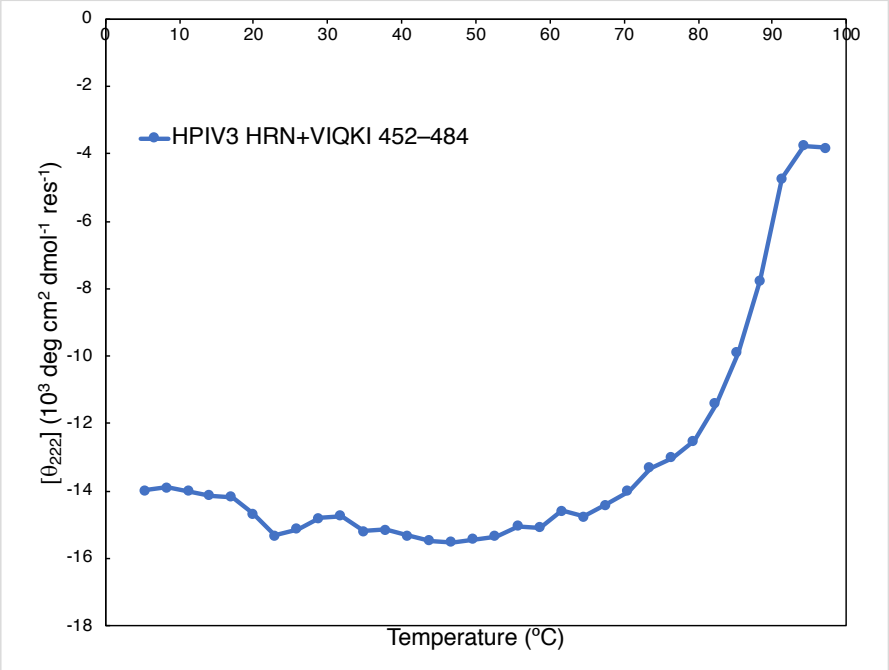

Figure S51 Thermal denaturation of 1:1 mixture of HPIV3 HRN+VIQKI 452–484

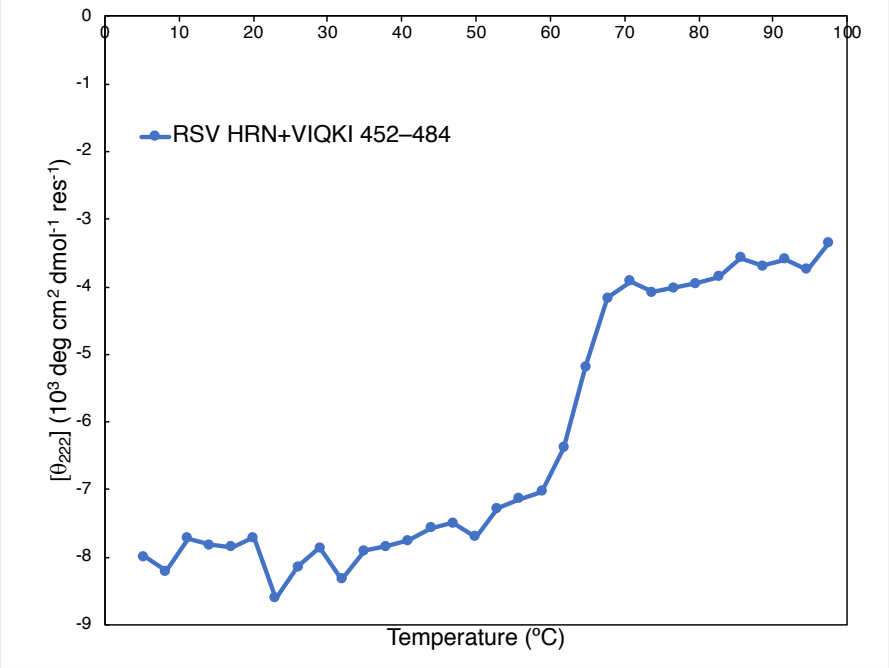

Figure S52 Thermal denaturation of 1:1 mixture of RSV HRN+VIQKI 452–484

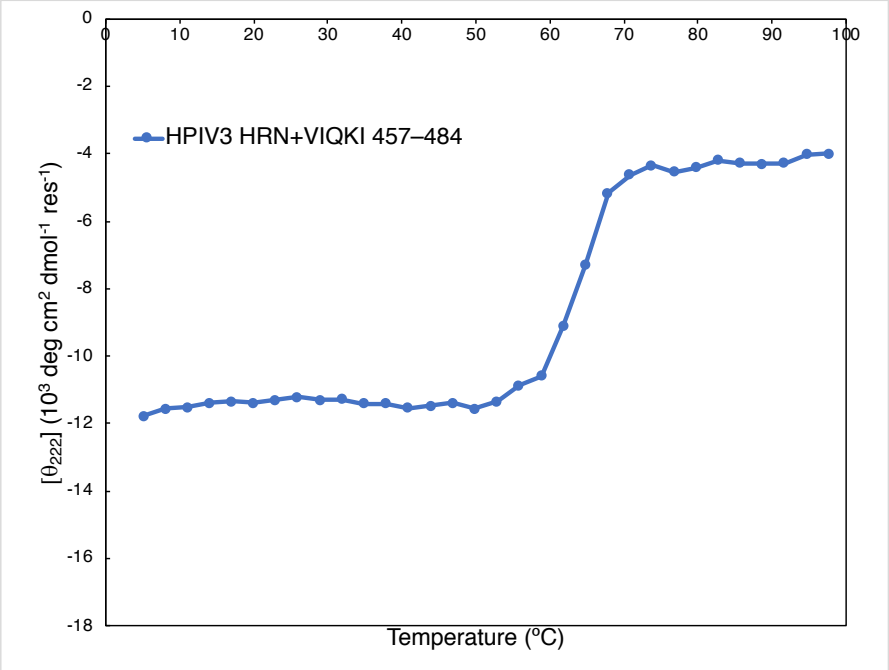

Figure S53 Thermal denaturation of 1:1 mixture of HPIV3 HRN+VIQKI 457–484

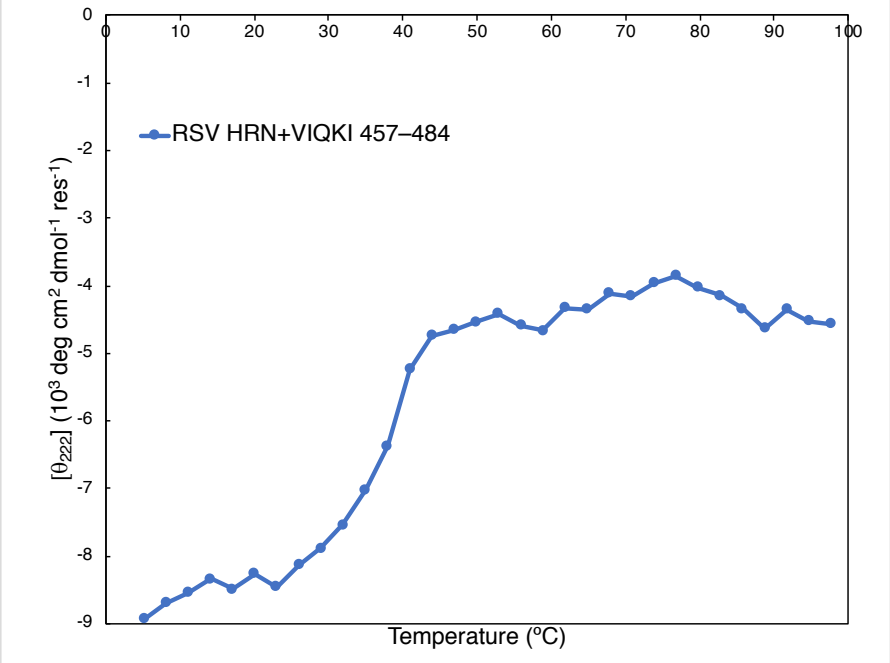

Figure S54 Thermal denaturation of 1:1 mixture of RSV HRN+VIQKI 457–484

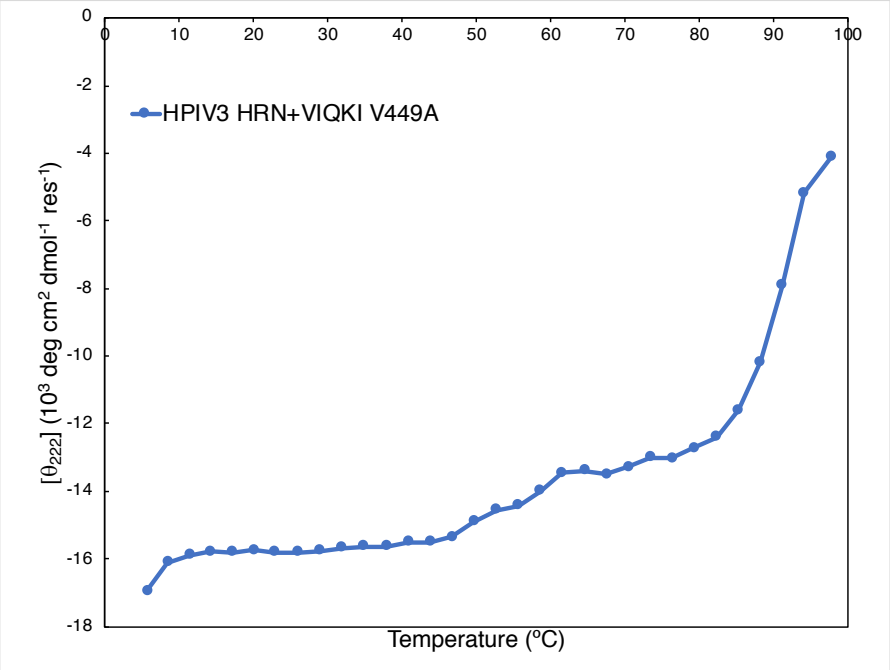

Figure S55 Thermal denaturation of 1:1 mixture of HPIV3 HRN+VIQKI V449A

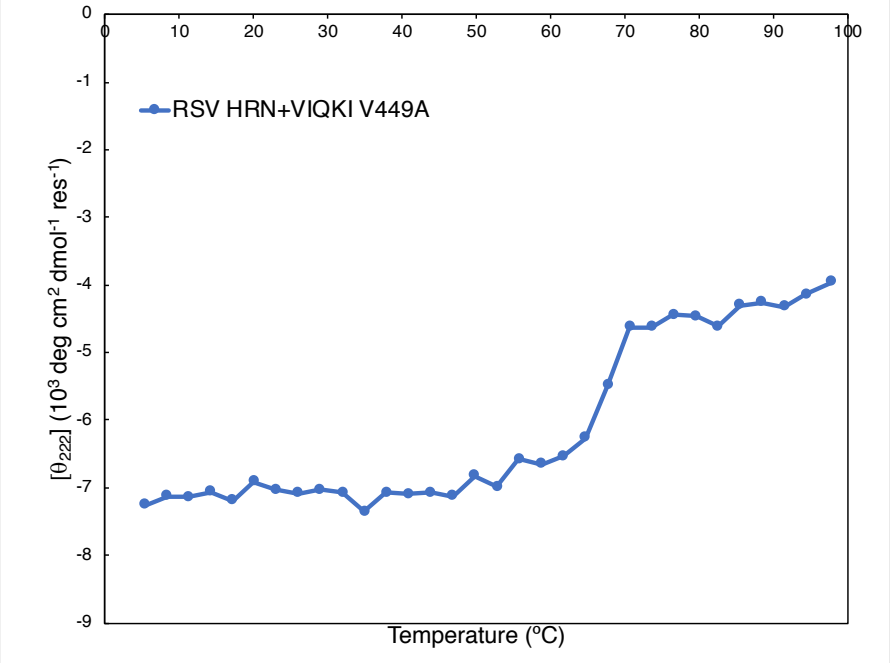

Figure S56 Thermal denaturation of 1:1 mixture of RSV HRN+VIQKI V449A

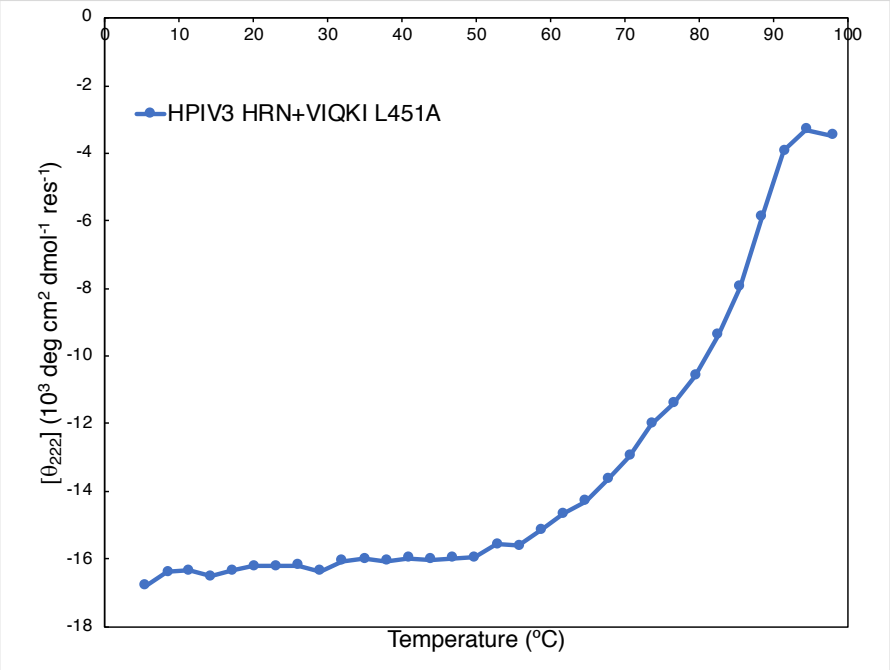

Figure S57 Thermal denaturation of 1:1 mixture of HPIV3 HRN+VIQKI L451A

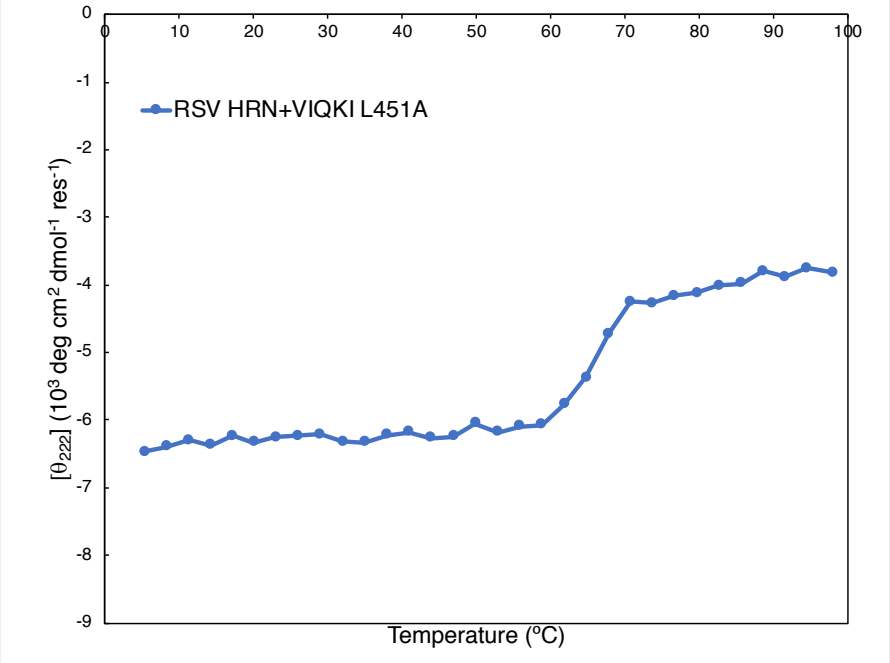

Figure S58 Thermal denaturation of 1:1 mixture of RSV HRN+VIQKI L451A

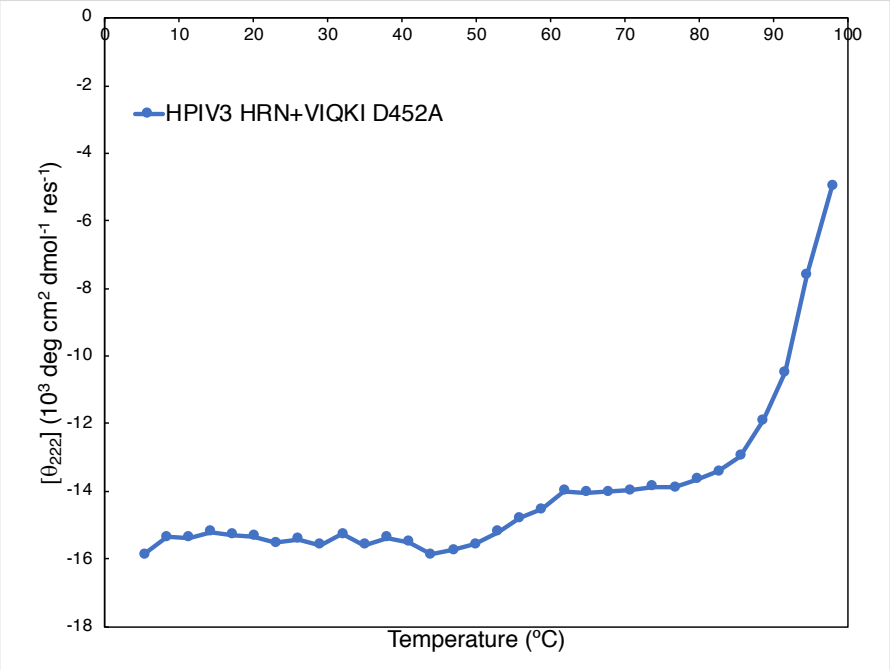

Figure S59 Thermal denaturation of 1:1 mixture of HPIV3 HRN+VIQKI D452A

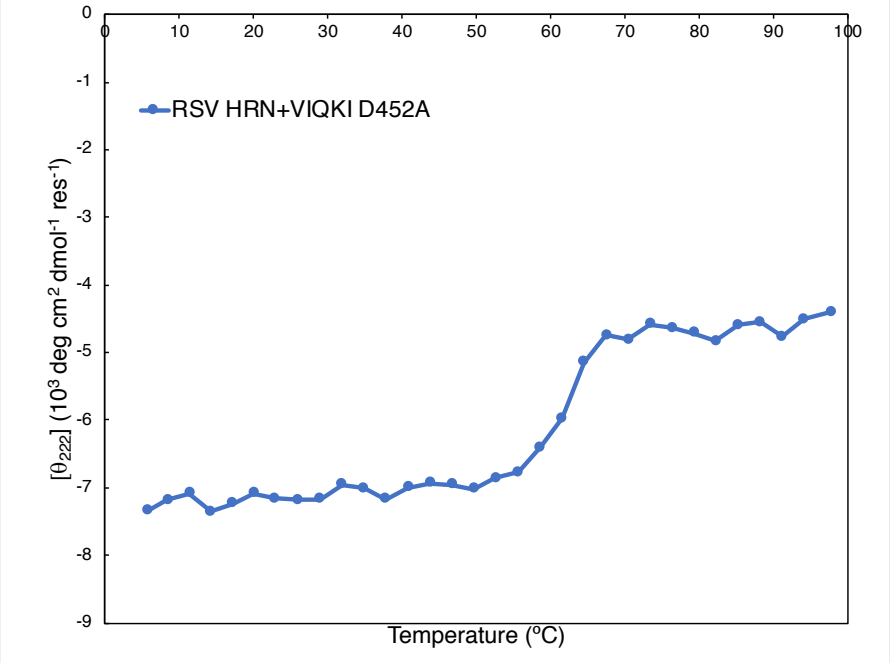

Figure S60 Thermal denaturation of 1:1 mixture of RSV HRN+VIQKI D452A

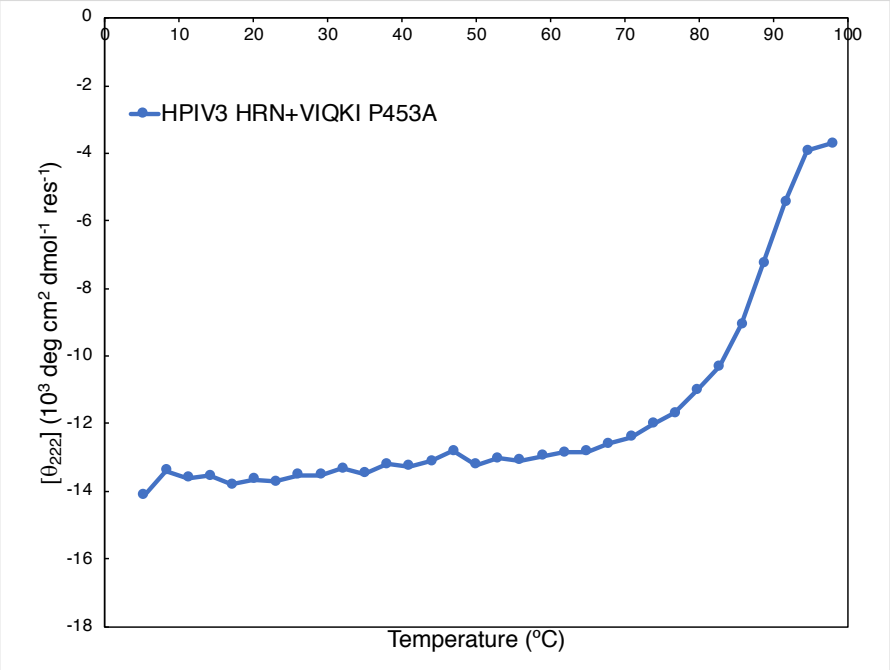

Figure S61 Thermal denaturation of 1:1 mixture of HPIV3 HRN+VIQKI P453A

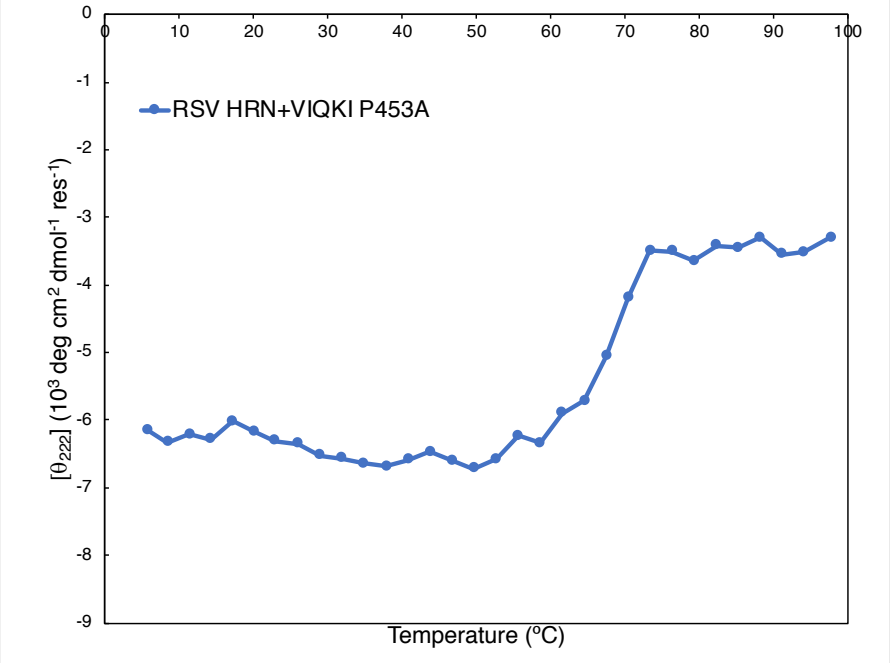

Figure S62 Thermal denaturation of 1:1 mixture of RSV HRN+VIQKI P453A

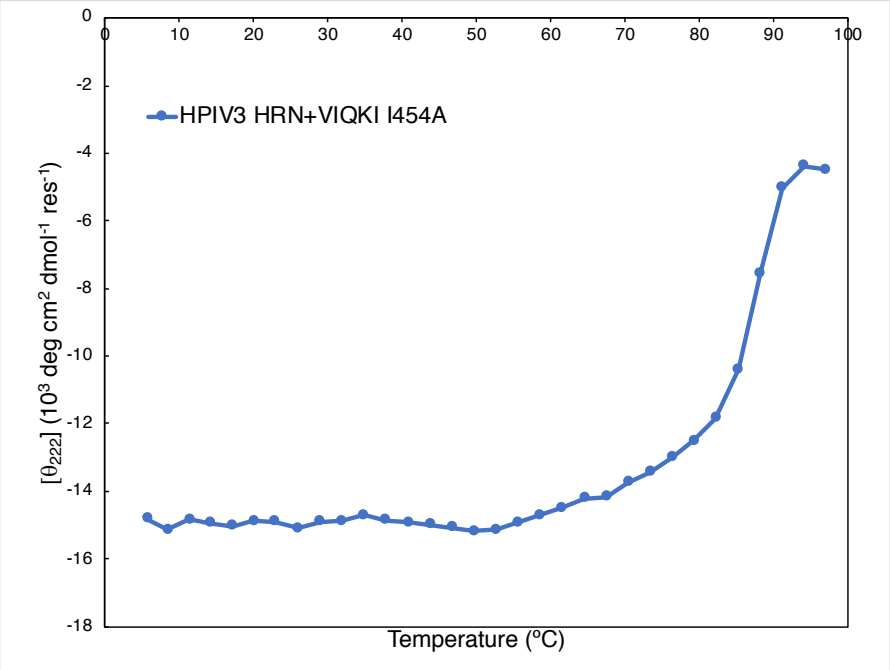

Figure S63 Thermal denaturation of 1:1 mixture of HPIV3 HRN+VIQKI I454A

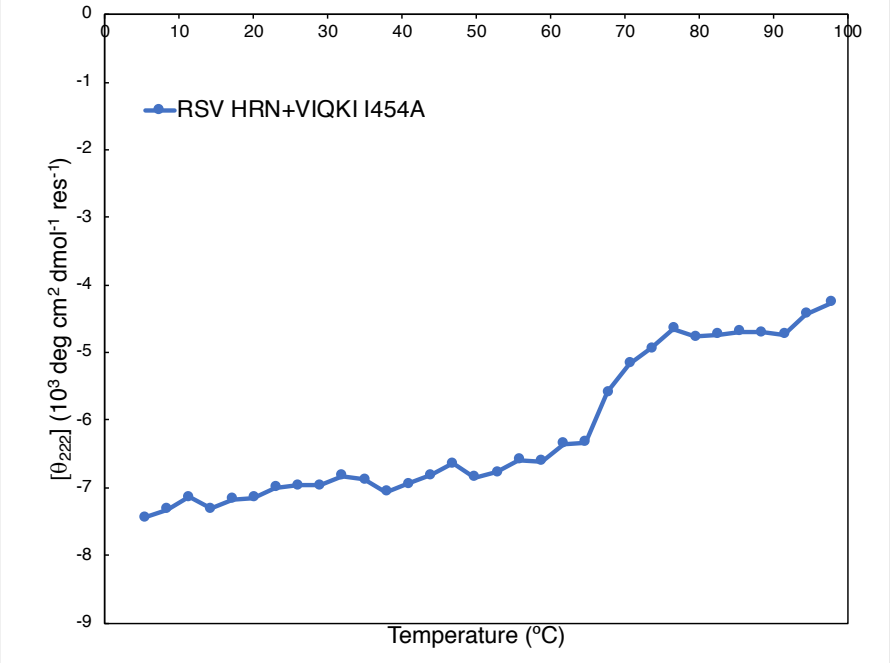

Figure S64 Thermal denaturation of 1:1 mixture of RSV HRN+VIQKI I454A

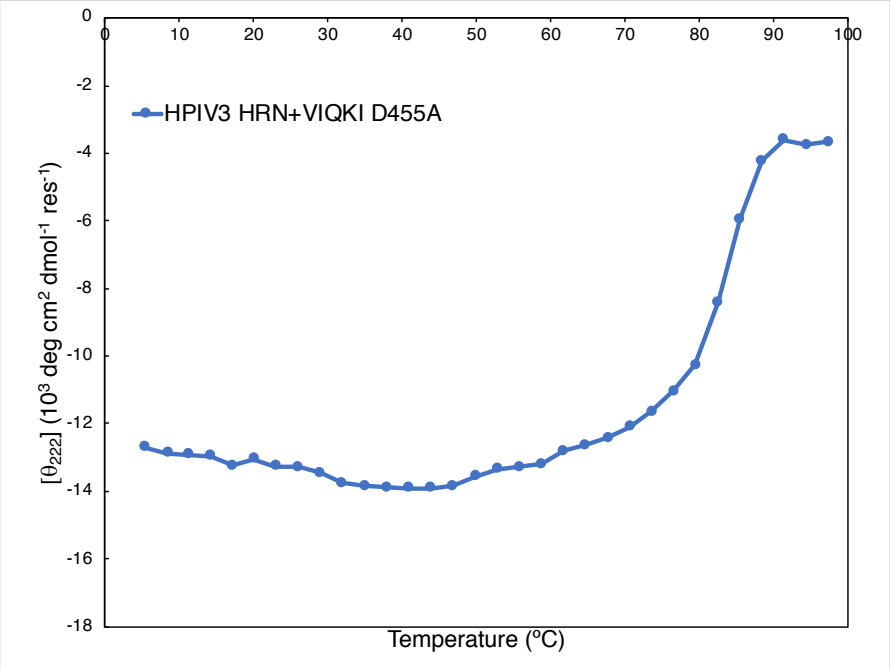

Figure S65 Thermal denaturation of 1:1 mixture of HPIV3 HRN+VIQKI D455A

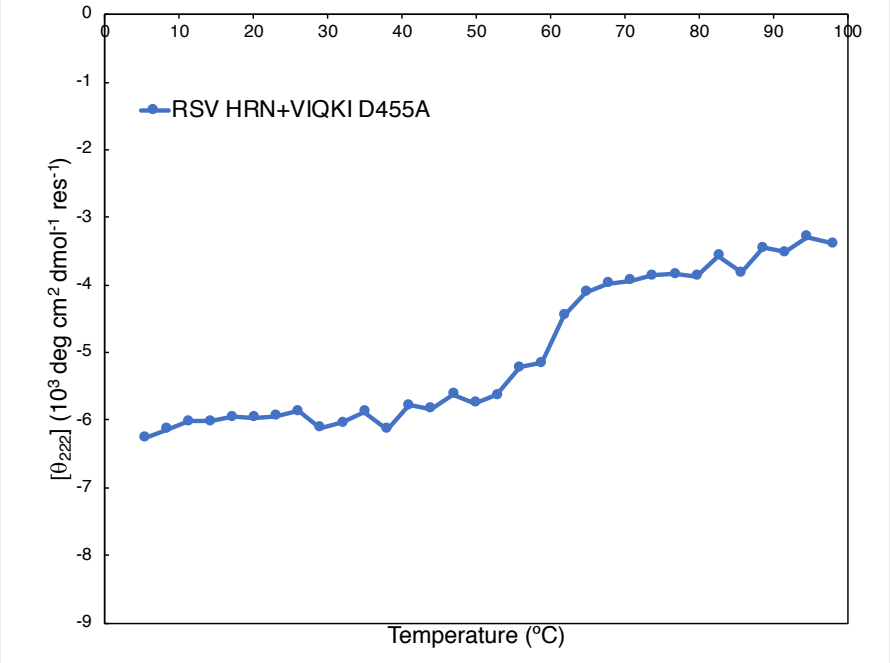

Figure S66 Thermal denaturation of 1:1 mixture of RSV HRN+VIQKI D455A

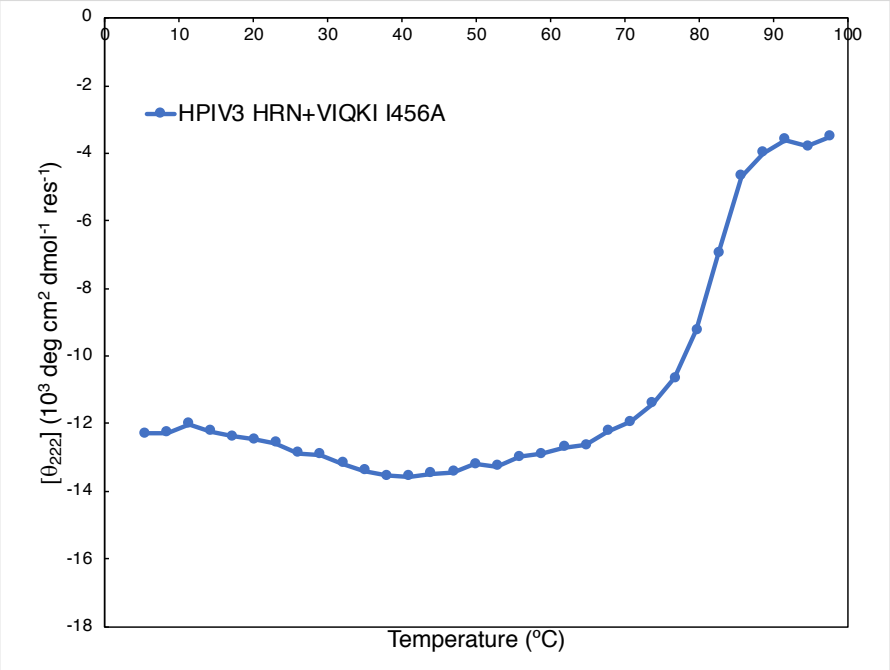

Figure S67 Thermal denaturation of 1:1 mixture of HPIV3 HRN+VIQKI I456A

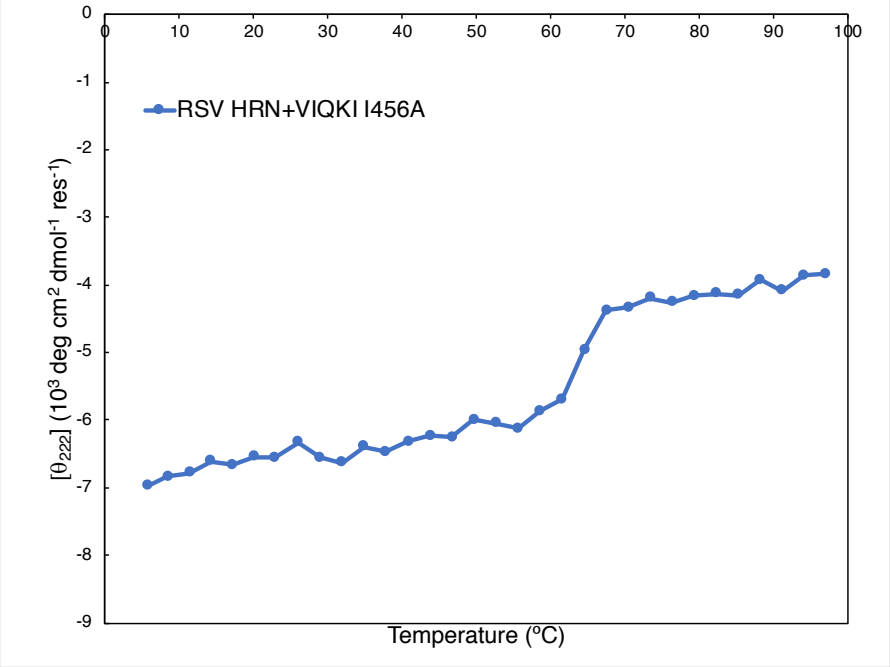

Figure S68 Thermal denaturation of 1:1 mixture of RSV HRN+VIQKI I456A

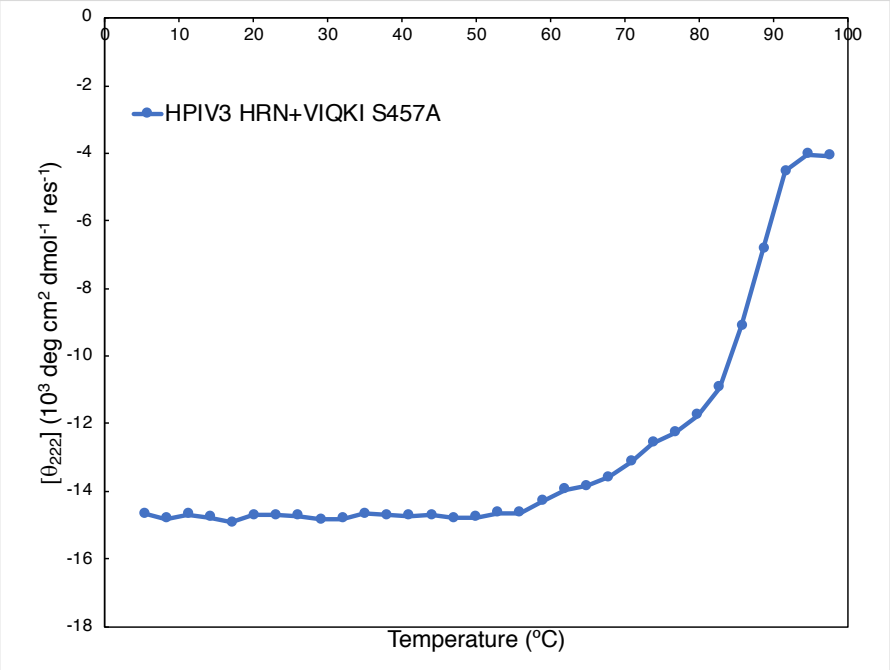

Figure S69 Thermal denaturation of 1:1 mixture of HPIV3 HRN+VIQKI S457A

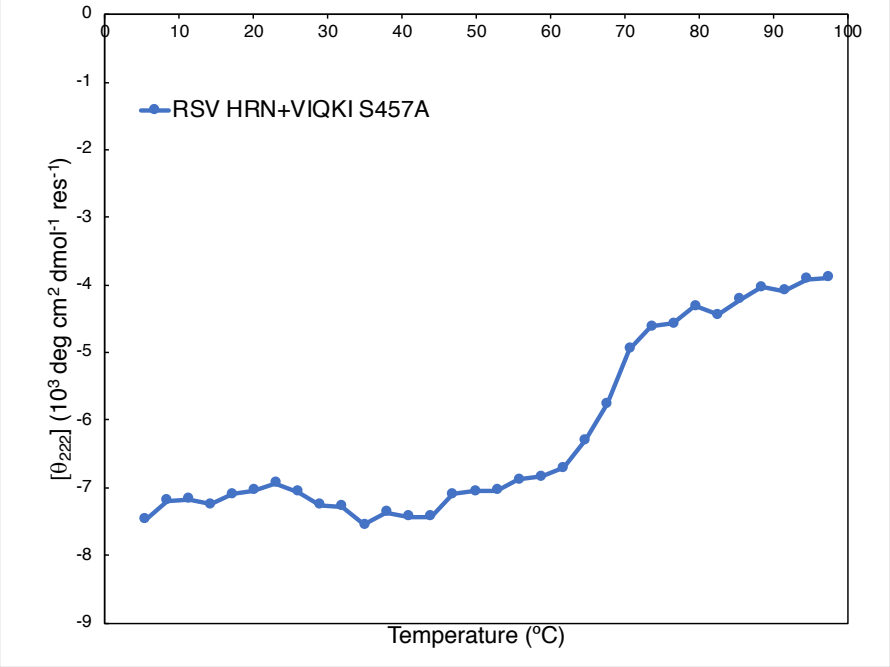

Figure S70 Thermal denaturation of 1:1 mixture of RSV HRN+VIQKI S457A

Assessment of Peptide Efficacy

Peptide–Cholesterol Conjugates, Cells, and Viruses

Peptide-cholesterol conjugates were obtained from American Peptide Company. An additional linker GSGSGC sequence was added to the C-terminus of each peptide. The cholesterol moiety was attached using displacement of an α-bromoamide as shown in Fig S71.

Figure S71 Synthesis of cholesterol-conjugated peptides

HEK293T (human kidney epithelial), CV-1 and Vero E6 cells were obtained from ATCC and were grown in Dulbecco's modified Eagle's medium (DMEM; Gibco) supplemented with 10% fetal bovine serum and antibiotics at 37°C and 5% CO_2. All cells tested negative for mycoplasma in MycoAlert™ Mycoplasma Detection Kit (Lonza).

For RSV infections, recombinant red fluorescent protein (RFP)-expressing RSV A2 (rrRSV) was obtained from Mark Peeples. rrRSV was generated from the full-length RSV plasmid MP224 by replacing the enhanced green fluorescent protein gene with the wild-type Discosoma RFP gene from pDsRed. For cell maintenance, HEp-2 cells (ATCC no. CCL-23) and Vero cells (ATCC no. CCL-81) were grown as monolayers and maintained in DMEM supplemented with 10% fetal calf serum (FCS) and 2 mM L-glutamine in a humidified atmosphere with 5%CO_2 at 37 °C. Viral stocks were prepared in HEp-2 cells (ATCC no. CCL-23). Briefly, HEp-2 cells were grown overnight, washed with OptiMEM, and inoculated with rrRSV. After a 2.5-h adsorption period the cells were incubated for 3 days in DMEM supplemented with 1% FCS. Virus was harvested by one freeze-thaw cycle followed by a clarifying centrifugation at 3,500 r.p.m. and stored at -80 °C. Viral titers were determined by plaque assay in Vero cells using a 2% methyl cellulose overlay, 5% (v/v) formaldehyde fixation, and crystal violet staining (0.015% w/v) at 5 days. To quantify the effects of peptides on RSV viral entry, Vero cell monolayers grown in 12-well plates were incubated for 180 min with rrRSV virus at a multiplicity of infection (MOI) of 6.7x10-4 in medium containing various concentrations of inhibitors. The media was discarded and replaced by methylcellulose. The dishes were incubated at 37°C for 72 h, and the crystal violet-stained plaques were counted.

For HPIV3, clinical isolate virus (CI) was obtained from the Clinical Microbiology Laboratories at New York Presbyterian Hospital and grown in human airway epithelium (HAE) at an air-liquid interface for only one passage prior to use in these experiments.[1,2]

Plasmids and Reagents

cDNA for the wild-type RSV F in pCAGGS was obtained from Mark Peeples.[3] HPIV3 HN and F genes from laboratory strains and clinical isolate viruses were cloned into pCAGGS mammalian expression vectors. Transfections in 293T cells were performed with Lipofectamine 2000 according to the manufacturer's protocols (Invitrogen).

β-Galactosidase Complementation-based Fusion Assay

We previously adapted a fusion assay based on alpha complementation of β-galactosidase (β-Gal).[4,5] In this assay, receptor-bearing cells expressing the omega peptide of β-Gal are mixed with cells co-expressing envelope glycoproteins and the alpha peptide of β-Gal, and cell fusion leads to alpha-omega complementation. Fusion is stopped by lysing the cells and, after addition of the substrate (®The Tropix Galacto-Star™ chemiluminescent reporter assay system, Applied Biosystem), fusion is quantified on a Spectramax M5 microplate reader. In the overnight fusion assay, cells expressing both alpha and omega peptides of β-Gal were co-cultured for up to 20 h.

Antiviral Activity against Live HPIV3 and rrRSV

Peptide activity against HPIV3 and rrRSV was determined by plaque reduction assays in infected cell monolayers and have been described previously.[1]

Peptide Efficacy Assessment in HAE Cultures

The EpiAirway AIR-100 system (MatTek Corporation) consists of normal human-derived tracheo/bronchial epithelial cells that have been cultured to form a pseudostratified, highly differentiated mucociliary epithelium closely resembling that of epithelial tissue in vivo. Upon receipt from the manufacturer, HAE cultures were transferred to 6-well plates (containing 0.9 ml medium per well) with the apical surface remaining exposed to air and incubated at 37°C in 5% CO_2.

HAE cultures were infected by applying 100 μl of EpiAirway medium containing 4,000 PFU of HPIV3 or rrRSV in the absence or presence of inhibitory peptide (10 μM) to the apical surface for 90 min at 37°C. The medium containing the inoculum was removed, and cultures were placed at 37°C and fed each day with 0.9 ml medium via the basolateral surface. Viruses were harvested by adding 200 μl medium per well to the HAE cultures' apical surface and allowed to equilibrate for 30 min at 37°C. The suspension was then collected, and viral titers were determined as previously described.[1]

X-ray Crystallography

Crystallization Conditions

Separate stock solutions of the HPIV3 HRN, RSV HRN, VI, and VIQKI peptides were prepared by dissolving the lyophilized peptide powder in water. Peptide concentration was measured by UV absorbance using tryptophan and tyrosine as the chromophores. Co-crystallization solutions were then prepared by mixing equal molar amounts of the relevant individual peptide solutions. Crystals were grown using hanging drop vapor diffusion. A 2 μL drop that comprised a 1:1 mixture of co-crystallization solution and the crystallization condition was placed on a glass cover slide that was then inverted to seal a well containing 150 μL of the crystallization condition. The crystallization conditions are given below.

- HPIV3 HRN+VI: 30 mM NaF, 30 mM NaBr, 30 mM NaI, 20% (v/v) PEG 500 MME, 10% (w/v) PEG 20000 in 100 mM imidazole/MES monohydrate buffer (pH 6.5)
- HPIV3 HRN+VIQKI: 30 mM $MgCl_2 \cdot 6H_2O$, 30 mM $CaCl_2 \cdot 2H_2O$, 12.5% (v/v) 2-methyl-2,4-pentanediol, 12.5% (v/v) PEG 1000, 12.5% (w/v) PEG 3350 in 100 mM NaHEPES/MOPS buffer (pH 7.5)
- RSV HRN+VIQKI: 30 mM NaF, 30 mM NaBr, 30 mM NaI, 12.5% (v/v) 2-methyl-2,4-pentanediol, 12.5% (v/v) PEG 1000, 12.5% (w/v) PEG 3350 in 100 mM NaHEPES/MOPS buffer (pH 7.5)

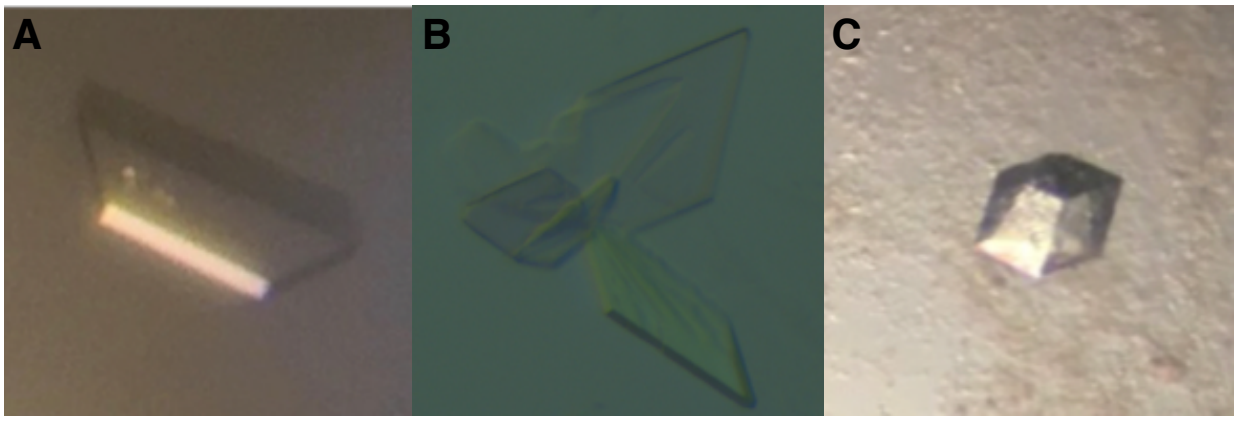

Figure S72 Crystal morphologies for (A) HPIV3 HRN+VI, (B) HPIV3 HRN+VIQKI, and (C) RSV HRN+VIQKI

X-ray Data Collection

Crystals were looped and vitrified in liquid nitrogen. Diffraction data for HPIV3 HRN+VI were collected at the Life Sciences Collaborative Access Team (LS-CAT) beam line 21-ID-G at the Advanced Photon Source (APS) at Argonne National Laboratory (ANL). Diffraction data for HPIV3 HRN+VIQKI were collected at the General Medical Sciences and Cancer Institutes Structural Biology Facility (GM/CA) at APS at ANL. Diffraction Data for RSV HRN+VIQKI were collected using a Bruker AXS MICROSTAR generator housed and maintained at the University of Wisconsin in the lab of Professor Katrina Forest.

- HPIV3 HRN+VI: LS-CAT 21-ID-G
- HPIV3 HRN+VIQKI: GM/CA 23-ID-B
- RSV HRN+VIQKI: Bruker AXS MICROSTAR

Data Processing, Structure Solution, and Refinement

Data were indexed and integrated using the program *XDS*. Data were then scaled and merged using the program *XSCALE*.[6] A molecular replacement solution was found with the program *Phaser* for each dataset using a poly-alanine dimeric model of the C-terminal and N-terminal heptad repeat regions from the postfusion HPIV3 F ectodomain (PDB: 1ZTM) as a search model. Model refinement was carried out using the program *phenix.refine* in combination with manual real-space model building and refinement in the program *Coot*.[7,8]

Table S1. HPIV3 HRN:VI (PDB: 6NYX)

Data collection	
X-ray source	APS 21-ID-G
X-ray detector	MAR300
Detector distance (mm)	250
Oscillation range (°)	0.2
Wavelength (Å)	0.97856
Space group	P 3
a / b / c (Å)	88.0 / 88.0 / 75.8
α / β / γ (°)	90 / 90 / 120
Volume (Å^3)	508000
Matthews coefficient (Å^3/Da)	2.00
Solvent content (%)	38.48
Resolution range (Å)	38.12–1.85 (1.916–1.85)
Number of observations	320426 (30469)
Unique reflections	56066 (5640)
Completeness	99.82% (99.96%)
Redundancy	5.7 (5.4)
Mean $I/\sigma(I)$	12.85 (1.35)
CC1/2*	0.99 (0.66)
R_{merge}	0.06986 (1.132)
R_{meas}	0.07694 (1.254)
R_{pim}	0.03216 (0.5373)
Wilson B-factor (Å^2)	31.14
Refinement statistics	
Refinement program	Phenix.refine: 1.13-2998
Non-hydrogen protein atoms refined	6099
Resolution range (Å)	38.12–1.85 (1.916–1.85)
No. of reflections used in refinement	55987 (5638)
Completeness (%)	99.83% (99.96%)
Reflections in cross-validation set	1693
R-value (work)	19.8
R-value (free)	22.9
R-value (overall)	19.9
Coordinate error (ML, Å)	0.24
Mean ADP (Å^2)	45.67
RMSD	
Bond lengths (Å)	0.018
Bond angles (°)	1.56

Table S2. HPIV3 HRN:VIQKI (PDB: 6NRO)

Data collection	
X-ray source	APS 23-ID-B
X-ray detector	Dectris Eiger X 16M
Detector distance (mm)	200
Oscillation range (°)	0.2
Wavelength (Å)	1.033
Space group	P 1 2_1 1
a / b / c (Å)	39.9 / 52.3 / 54.1
α / β / γ (°)	90.0 / 100.6 / 90.0
Volume ($Å^3$)	111000
Matthews coefficient ($Å^3$/Da)	1.88
Solvent content (%)	34.6
Resolution range (Å)	39.29–1.75 (1.813–1.75)
Number of observations	145854 (14339)
Unique reflections	22158 (2189)
Completeness	99.50% (99.95%)
Redundancy	6.6 (6.5)
Mean $I/\sigma(I)$	18.26 (1.45)
CC1/2*	1.00 (0.73)
R_{merge}	0.0449 (1.139)
R_{meas}	0.0489 (1.238)
R_{pim}	0.0193 (0.480)
Wilson B-factor ($Å^2$)	36.71
Refinement statistics	
Refinement program	Phenix.refine: 1.13-2998
Non-hydrogen protein atoms refined	2014
Resolution range (Å)	39.29–1.75 (1.813–1.75)
No. of reflections used in refinement	22122
Completeness (%)	99.50% (99.95%)
Reflections in cross-validation set	1997
R-value (work)	21.7
R-value (free)	24.4
R-value (overall)	21.9
Coordinate error (ML, Å)	0.25
Mean ADP ($Å^2$)	54.3
RMSD	
Bond lengths (Å)	0.016
Bond angles (°)	1.48

Table S3. RSV HRN:VIQKI (PDB: 6NTX)

Data collection	
X-ray source	Bruker AXS MICROSTAR
X-ray detector	Bruker SMART 6000
Detector distance (mm)	50
Oscillation range (°)	1.0
Wavelength (Å)	1.5418
Space group	R32:H
a / b / c (Å)	52.0 / 52.0 / 299.0
α / β / γ (°)	90 / 90 / 120
Volume (Å^3)	700000
Matthews coefficient (Å^3/Da)	1.99
Solvent content (%)	38.2
Resolution range (Å)	28.76–2.20 (2.279–2.20)
Number of observations	166585 (14005)
Unique reflections	8390 (829)
Completeness	99.67% (99.64%)
Redundancy	19.9 (16.9)
Mean $I/\sigma(I)$	15.34 (2.43)
CC1/2*	0.998 (0.863)
R_{merge}	0.1259 (1.596)
R_{meas}	0.1297 (1.645)
R_{pim}	0.03028 (0.3936)
Wilson B-factor (Å^2)	39.90
Refinement statistics	
Refinement program	Phenix.refine: 1.13-2998
Non-hydrogen protein atoms refined	1047
Resolution range (Å)	28.76–2.20 (2.279–2.20)
No. of reflections used in refinement	8371
Completeness (%)	99.7 (99.7)
Reflections in cross-validation set	837
R-value (work)	23.2
R-value (free)	28.5
R-value (overall)	23.7
Coordinate error (ML, Å)	0.27
Mean ADP (Å^2)	56.89
RMSD	
Bond lengths (Å)	0.014
Bond angles (°)	1.46

References

1. Palmer, S. G.; DeVito, I.; Jenkins, S. G.; Niewiesk, S.; Porotto, M.; Moscona, A. Circulating Clinical Strains of Human Parainfluenza Virus Reveal Viral Entry Requirements for in Vivo Infection. *J. Virol.* **2014**, *88* (22), 13495–13502.
2. Palermo, L. M.; Uppal, M.; Skrabanek, L.; Zumbo, P.; Germer, S.; Toussaint, N. C.; Rima, B. K.; Huey, D.; Niewiesk, S.; Porotto, M.; Moscona, A. Features of Circulating Parainfluenza Virus Required for Growth in Human Airway. *mBio* **2016**, *7* (2), e00235–11.
3. Branigan, P. J.; Liu, C.; Day, N. D.; Gutshall, L. L.; Sarisky, R. T.; Del Vecchio, A. M. Use of a Novel Cell-Based Fusion Reporter Assay to Explore the Host Range of Human Respiratory Syncytial Virus F Protein. *Virol. J.* **2005**, *2*, 54.
4. Moosmann, P.; Rusconi, S. Alpha Complementation of LacZ in Mammalian Cells. *Nucleic Acids Res.* **1996**, *24* (6), 1171–1172.
5. Porotto, M.; Fornabaio, M.; Kellogg, G. E.; Moscona, A. A Second Receptor Binding Site on Human Parainfluenza Virus Type 3 Hemagglutinin-Neuraminidase Contributes to Activation of the Fusion Mechanism. **2007**, *81* (7), 3216–3228.
6. Kabsch, W. (2010) Integration, scaling, space-group assignment and post-refinement. *Acta Crystallogr D Biol Crystallogr* 66:125-132.
7. Adams, P. D.; Afonine, P. V.; Bunkóczi, G.; Chen, V. B.; Davis, I. W.; Echols, N.; Headd, J. J.; Hung, L.-W.; Kapral, G. J.; Grosse-Kunstleve, R. W.; McCoy, A. J.; Moriarty, N. W.; Oeffner, R.; Read, R. J.; Richardson, D. C.; Richardson, J. S.; Terwilliger, T. C.; Zwart, P. H. PHENIX: a Comprehensive Python-Based System for Macromolecular Structure Solution. *Acta Crystallogr. D Biol. Crystallogr.* **2010**, *66* (2), 213–221.
8. Emsley, P.; Cowtan, K. Coot: Model-Building Tools for Molecular Graphics. *Acta Crystallogr. D Biol. Crystallogr.* **2004**, *60* (Pt 12 Pt 1), 2126–2132.